AD

USAAVSCOM TECHNICAL REPORT 72-4

TWO METHODS OF PREDICTION OF HOVERING PERFORMANCE

BY

HAROLD Y. H. LAW

D D C

MAR 20 1972

C

FEBRUARY 1972

DIRECTORATE OF RESEARCH, DEVELOPMENT, AND ENGINEERING
US ARMY AVIATION SYSTEMS COMMAND
ST. LOUIS, MISSOURI

DOCUMENT CONTROL DATA - R & D

(Security classification of title, body of abstract and indexing annotation must be entered when the overall report is classified)

1. ORIGINATING ACTIVITY *(Corporate author)*	2a. REPORT SECURITY CLASSIFICATION
Flight Standards and Qualification Division Directorate for RD&E	UNCLASSIFIED
	2b. GROUP N/A

3. REPORT TITLE

Two Methods of Prediction of Hovering Performance

4. DESCRIPTIVE NOTES *(Type of report and inclusive dates)*

Technical

5. AUTHOR(S) *(First name, middle initial, last name)*

Harold Y.H. Law

6. REPORT DATE	7a. TOTAL NO. OF PAGES	7b. NO. OF REFS
February 1972	75	17

8a. CONTRACT OR GRANT NO.	9a. ORIGINATOR'S REPORT NUMBER(S)
b. PROJECT NO.	TR 72-4
c.	9b. OTHER REPORT NO(S) *(Any other numbers that may be assigned this report)*
d.	ADS TN 69-1

10. DISTRIBUTION STATEMENT

Unlimited

11. SUPPLEMENTARY NOTES	12. SPONSORING MILITARY ACTIVITY
	USAAVSCOM

13. ABSTRACT

This report presents two methods of prediction on the hovering performance of single-rotor helicopters. A generalized equation was formulated by the use of numerical and empirical techniques from flight test data for the prediction of hovering performance. This generalized equation leads to two methods of prediction: the Generalized Method and the Two-Point Method. Both of these methods of prediction are simple and easy to apply, and require only limited flight data information to predict the entire range of hovering performance. Furthermore, the accuracy of these methods is within 5% of the flight data. Specific working examples and procedures are given in the appendix.

DD FORM 1473 REPLACES DD FORM 1473, 1 JAN 64, WHICH IS OBSOLETE FOR ARMY USE.

14. KEY WORDS	LINK A		LINK B		LINK C	
	ROLE	WT	ROLE	WT	ROLE	WT
Hovering performance of helicopter						

73

DISCLAIMER

The findings in this report are not to be construed as an official Department of the Army position unless so designated by other authorized documents.

/

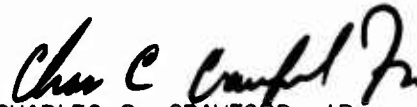# TWO METHODS OF PREDICTION OF HOVERING PERFORMANCE

By
Harold Y. H. Law

February 1972

PREFACE

Under AMC Regulation No. 70-32, the Flight Standards and Qualification
Division, US Army Aviation Systems Command is responsible for the development,
promulgation and application of Aeronautical Design Standards (ADS) for
US Army Aircraft Systems. As part of this responsibility, a series of
Aeronautical Design Standards Technical Notes will be published to provide
substantiation for proposed standards, revisions and related studies. This
report constitutes a portion of this series.

CHARLES C. CRAWFORD, JR.
Chief of Flight Standards
and Qualification Division

TABLE OF CONTENTS

SUMMARY

This report presents two methods of prediction on the hovering performance
of single-rotor helicopters. Flight test data of ten helicopters (Bell 47 J-2,
UH-12E-4, YH-40, YHO-2HU, YUH-ID (48 ft. rotor), YUH-ID (44 ft. rotor), YHU-IB,
UH-IC, CH-54A, and CH-47A) including one tandem, with solidity ranging from
0.030 to 0.105, gross weight from 1,550 to 38,000 lbs. and rotor diameter
from 25 to 72 feet were investigated in this study. All the above aircrafts
were tested within the past ten years.

By the use of numerical and empirical techniques, a generalized equation
was formulated for the prediction of hovering performance. This generalized
equation leads to two methods of prediction: the Generalized Method and the
Two-Point Method.

The outstanding features of these two methods of prediction are first
of all that they are simple and easy to apply. Secondly, they both require
only limited flight data information (OGE C_P - C_T or one IGE skid height
C_P - C_T data) to predict the entire range of hovering performance, thus
reducing the time, manhours, and therefore the cost of flight tests. Thirdly,
they provide accurate predictions within 5% from the flight data. The Two-
Point Method requires additional flight data, however it provides better
accuracy than the Generalized Method.

Both of these methods were tested on the helicopters in this study and
also on four other helicopters not included in this study. The results
show that in all cases, the prediction of the relative thrust increase is
within 5% deviation from the flight test data.

These two methods are flexible in their applications and can be success-
fully employed in the following areas of prediction:

(1) a. Prediction of relative thrust increase ($C_T/C_{T\infty}$), given
only aircraft dimensional characteristics.

b. Prediction of relative thrust increase ($C_T/C_{T\infty}$), given OGE.

(2) Prediction of IGE performance, given OGE flight data.

(3) Prediction of IGE performance, given predicted OGE performance
by analytical formulation.

(4) Prediction of OGE and the rest of IGE performance, given one
skid height IGE flight data.

(5) Prediction of IGE performance, given OGE and one low and one
high power level flight data at various IGE. (Two-Point
Method).

The last area of application suggests a new method of flight test, which is to fly on two constant power (C_p) levels with one high and one low power at various IGE skid heights.

The major portion of this report is to present the mathematical model and approaches, motivations, justification, discussions, and comparison with the flight data of these methods. Those who are interested in the working of these methods can refer to Appendix A for specific applications and procedures.

I. INTRODUCTION

The ground effect on a lifting airscrew was treated both mathematically and experimentally by Knight and Hefner (Reference I) in 1941. Experimental results were also reported by Zbrozek (Reference 2) in 1947. A summary of these results is presented by Gessow and Myers (Reference 3) in their book "Aerodynamics of the Helicopter."

In Zbrozek's experimental investigation, some twenty-five different rotor blades were used with various rotational speeds, number of blades, profile drags, shapes of blades, blade twists, and pitch settings. It was concluded by Zbrozek that the relative increase of lift $(C_T/C_{T\infty})^*$, at constant power depends mainly on (I) relative rotor height above ground, (Z/D) and (2) mean lift coefficient of the blade, C_L, which can be expressed in terms of power level, $C_{T\infty}/\sigma$. Rotational speed, number of blades, profile drag, and shape of blade exert only a minor influence on the increase in lift.

The experimental conclusion obtained by Zbrozek was based on static tests. For more realistic and up-to-date results, one needs to go into flight test of recent helicopters. With this in mind, the ground effect was reinvestigated by using recent flight test data.

Flight test data of the following helicopters, Bell 47 J-2, UH-12E-4, YH-40, YHO-2HU, YUH-ID (48 ft. rotor), YUH-ID (44 ft. rotor), YHU-IB, UH-IC CH-54A, and CH-47A were collected and used in this study. The objective of this study is to find a method which will predict the relative thrust increase within a desired accuracy (5% deviation) without going into extensive and elaborate full-scale flight testing. Such a method of prediction is therefore useful not only in preliminary design, but also in predicting the hovering performance accurately, which will result in the saving of time and cost of flight test.

The purpose of this report is to present such a method of prediction along with the verification of its accuracy and flexibility of application. In this report, major effort has been devoted to the study of single-rotor type helicopters. However, the strictly tandem type helicopters could also be treated in a similar manner as presented here upon the availability of sufficient flight test data.

---

*Refer to page 28 for definitions for symbols

I

2. METHOD AND APPROACH

An empirical relationship illustrating the effect of rotor height on rotor thrust produced at constant power was concluded by Zbrozek and is presented in Figure I. The approach of this study is to employ the currently available flight test data to reassess the relationship shown in Figure I by use of numerical techniques.

2.1 Mathematical Model

The aim of this model is to simulate the relationship between relative thrust ($C_T/C_{T\infty}$) and relative rotor height (Z/D) at constant power levels ($C_{T\infty}/\sigma$) during hover. It is important to keep in mind that any experimental observations have inherent errors associated with them. These errors may be caused by instrumentations, external testing environment, or by the observer himself. They are generally not known and their causes may be different in each case. Therefore the approach of modeling is not to simulate each individual test case independently from other cases, but to simulate the general trends which are revealed from the available flight data of all helicopters considered in this study. From these general trends, a general expression and a method can be formulated to provide a close prediction of hovering performance for single-rotor type helicopters. This mathematical model should be simple and should provide close simulation to experimental results; and the methods of prediction resulting from this model should be easy to apply.

It is assumed here that the errors in the flight test data in this study follow the Gaussian distribution. This assumption will be substantiated later in this study. Then the principle of least squares and the statistical treatments can be meaningfully applied in the mathematical manipulations which are to follow in the course of this study.

2.2 Selection of Empirical Function

The recent flight test data and the results obtained by Zbrozek both suggest that the functional relationship between $C_T/C_{T\infty}$ and Z/D at constant $C_{T\infty}/\sigma$ is hyperbolic. This relation can be observed from Figure 2 through Figure II. The objective is to select a general mathematical expression which can best represent the trend of this relationship. A logical way to implement this is to try the simplest types of functional relations first. A few of such relations were attempted to achieve this goal. They are listed below:

(1) power function: $Y = aX^b$

(2) First hyperbolic function: $Y = \dfrac{aX + b}{X}$

(3) Second hyperbolic function: $Y = \dfrac{X}{aX + b}$

where a and b are constants.

2

In this case Z/D and $C_T/C_{T\infty}$ are represented by X and Y respectively. It was found that the second hyperbolic function best represents the flight data. Therefore, this form was used to obtain empirical expressions for all helicopters investigated herewith. A comparison of the different types of functions to simulate the data of the YHU-IB helicopter is shown in Figure 12. Discussion on the suitability of these empirical functions is presented in Appendix B.

2.3 Solving for the Constants

Having determined an empirical function that expresses the hovering performance at each power level in the form of

$$Y = \frac{X}{aX + b}$$

where $X = Z/D$, $Y = C_T/C_{T\infty}$,

the next step is to solve for the constants (a, b) of each helicopter at each power level so that this empirical function will best approximate the experimental result.

Let F_i be the functional values of the data, and y_i be the approximated values. In the least squares approximation, the quantity that needs to be minimized for the most probable values of y_i is

$$\sum_{i=1}^{m} (F_i - y_i)^2 \qquad (1)$$

where m = number of data points

To satisfy the above condition (1), the following must be true:

$$G_2 = \frac{\delta}{\delta b} \sum_{i=1}^{m} (F_i - y_i)^2 = 0 \qquad (2)$$

$$(3)$$

$$G_1 = \frac{\delta}{\delta a} \sum_{i=1}^{m} (F_i - y_i)^2 = 0$$

3

Expanding (2) and (3),

$$G_1 = \sum_{i=1}^{m} F_i \frac{X_i^2}{(aX_i + b)^2} - \sum_{i=1}^{m} \frac{X_i^3}{(aX_i + b)^3} = 0 \qquad (4)$$

$$G_2 = \sum_{i=1}^{m} F_i \frac{X_i}{(aX_i + b)^2} - \sum_{i=1}^{m} \frac{X_i^2}{(aX_i + b)^3} = 0 \qquad (5)$$

Now the values of (a, b) can be determined for all power levels by solving the two simultaneous equations (4) and (5) by the classical Newton-Raphson method (Reference 4).

2.4 Fitting of a and b

Since the relative thrust increase $C_T/C_{T\infty}$ is a strong function of Z/D and $C_{T\infty}/\sigma$ it can be assumed that a and b are strong functions of $C_{T\infty}/\sigma$. Now it is required to find the general trends of a and b as a whole with respect to $C_{T\infty}/\sigma$, so that expressions of a and b as functions of $C_{T\infty}/\sigma$ can be obtained.

To do so, the principle of least squares approximation with orthogonal polynomials is applied to obtain a close fit of the data. The expression of this polynomial is of the form

$$y(X) = C_0 + C_1 X + C_2 X^2 + C_3 X^3 + \ . \ . \ . \ + C_n X^n$$

where C_i, i = 0, 1, . . ., n, are constants, and y can be expressed as a or b, and X as $C_{T\infty}/\sigma$.

This method minimizes the sum of the squares of the deviations between the functional and the approximated values to give the most probable approximation.

Thus, the expressions of a and b with respect to $C_{T\infty}/\sigma$ can be written as

$$a = K_{10} + K_{11} \left(\frac{C_{T\infty}}{\sigma}\right) + K_{12} \left(\frac{C_{T\infty}}{\sigma}\right)^2 + \ldots + K_{1n} \left(\frac{C_{T\infty}}{\sigma}\right)^n$$

$$b = K_{20} + K_{21} \left(\frac{C_{T\infty}}{\sigma}\right) + K_{22} \left(\frac{C_{T\infty}}{\sigma}\right)^2 + \ldots + K_{2n} \left(\frac{C_{T\infty}}{\sigma}\right)^n$$

where K_{ij}, i = 1, 2, j = 0, 1, . . ., n, are constants.

4

2.5 Generalized Hovering Equation

Now knowing that $C_T/C_{T\infty}$ as a function of Z/D, a and b, and that a and b as functions of $C_{T\infty}/\sigma$, a generalized hovering equation can be obtained by expressing a and b in terms of $C_{T\infty}/\sigma$ in the hyperbolic relation. This generalized equation can now be written as

$$\frac{C_T}{C_{T\infty}} = \frac{Z/D}{[K_{10}+K_{11}(C_{T\infty}/\sigma)+...+K_{1n}(C_{T\infty}/\sigma)^n](Z/D) + [K_{20}+K_{21}(C_{T\infty}/\sigma)+...K_{2n}(C_{T\infty}/\sigma)^n]}$$

In this equation, the constants K_{ij}, can be calculated from the flight data and should be fixed for a certain type of helicopters. Once the relative skid height, Z/D, and the power level, $C_{T\infty}/\sigma$, are specified, the corresponding relative thrust increase $C_T/C_{T\infty}$, can be predicted.

The accuracy of simulation and the usage of this generalized equation will be discussed in Sections 3.7 and 3.8.

3. RESULTS AND DISCUSSIONS

3.1 Flight Test Data

In this study, the flight test data of the following aircrafts: (YUH-ID (48 ft. rotor), UH-IC, YH-40, YHU-IB, Bell 47 J-2, UH-12E-4, YHO-2HU, YUH-ID (44 ft. rotor), CH-54A, CH-47A) were employed (References 5 to 13). The detailed breakdown of the data is presented on Tables II to XI. The data were extracted from the C_P - C_T curves of the flight test results from as low as one foot skid height to the out-of-ground skid height. They were then reduced to the parameters $C_T/C_{T\infty}$, Z/D, and $C_{T\infty}/\sigma$ and are shown in Figures 2 to II.

These data represent a wide range of single-rotor helicopters (with one tandem) with the rotor solidity range from 0.030 to 0.105, and with the gross weight range from 1,550 lbs. to 38,000 lbs. The dimensional characteristics of these helicopters are presented on Table I. This diversity of helicopter categories which were tested within the past ten years may reduce the chances of bias toward any one type of helicopter. By so doing, a fair treatment can be performed on the prediction of hovering performances of a wide range of single-rotor helicopters.

One important understanding of the flight data needs to be pointed out here. Each of the C_P - C_T curves obtained from the performance reports (References 5 to 13) is a result of the hovering flight test at various rotor speeds and density altitudes, and also with slight influence of wind. There is in every case a spread of test data with a maximum of about 5% deviation from the mean [1]. A typical example of these C_P - C_T curves for the YHU-IB (Reference 7) hovering at 60 ft. skid height is shown in Figure 13. Therefore, an inherent 5% maximum error distribution is already

5

incorporated in the data to be used at the very outset. Due to this characteristic of flight data, it is therefore reasonable to accept a maximum of 5% deviation as the limit of tolerance in the prediction of hovering performance by the methods presented in this report.

3.2 Selection of Data

The trend of flight data as presented in Figures 2 to 11 needs first to be studied. A helicopter is considered hovering at OGE when the value of C_T/C_{T_∞} reaches 1. In other words, the ground effect at OGE has negligible influence on the relative thrust increase. As presented in the figures, it can be observed immediately that the data follow a hyperbolic trend very nicely until $C_T/C_{T_\infty} = 1$. From then on, the value of C_T/C_{T_∞} remains to be 1.0 as the value of Z/D increases. The figure below clarifies this point.
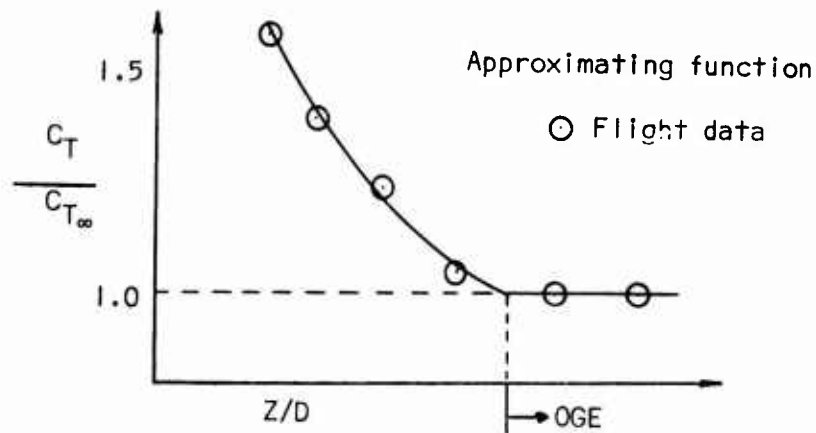
Because of the discontinuity of the hyperbola at OGE, the objective of fitting an empirical function through these data points is to obtain an expression that will best approximate the experimental result within the IGE region. With this criterion in mind, one therefore is lead to fit a curve through the IGE data points as closely as possible and put less emphasis on the OGE data in this process of curve fitting. The data beyond OGE tend to bias the approximating function, resulting in a larger deviation from the flight data. Using YUH-ID as an example, this influence on the least squares approximation by the data at and beyond OGE can be clearly observed in Figure 14.

3.3 Behavior of "a" and "b" as functions of C_{T_∞}/σ.

The values of a and b were plotted with respect to the constant power term C_{T_∞}/σ in Figures 15 and 16. The distribution of the values of a as presented in Figure 15 shows a definite linear relation with power levels.

_____

(1) It is not clear whether the hovering performance curves were drawn through the data points by the least squares method, or the method of averages, or simply by human judgment.

6

However, there is a scatter in the values of b with respect to power levels as presented in Figure 16. It is not immediately discernible as to what degre of polynomial is most suitable in fitting such data. Therefore, polynomials up to the third degree were attempted to approximate this relationship. It was then found that the differences were so minute that the approximating polynomials of the second and the third degree were essentially the same as that of the first degree. Thus a linear relationship between b and C_{T_∞}/σ was used in fitting through the data points. Hence, the linear functions of a and b with respect to C_{T_∞}/σ can be written in the form of

$$a = K_1 + K_2(C_{T_\infty}/\sigma)$$

$$\text{and} \quad b = K_3 + K_4(C_{T_\infty}/\sigma) \tag{3.1}$$

$$\text{where } K_1, K_2, K_3, K_4 \text{ are constants}$$

One phenomenon which can be readily observed from Figure 15 and 16 is that for each individual helicopter the values of a and b form linear or very close to linear relationship with the parameter C_{T_∞}/σ. Hence, to provide a closer prediction in the hovering performance, these individual linear relationships can be used instead of the linear functions obtained from the overall least squares fit. These individual linear functions retain the form of (3.1). However, the constants K's will be different for each helicopter. This observation of individual linear functions leads to the motivation of a new flight test method which will reduce the time and cost of flight testing and will be discussed in Section 3.6.

3.4 Generalized Equation of Prediction

The function of a and b with respect to C_{T_∞}/σ is linear as discussed in the previous section. Then the generalized equation of hovering performance can be simplified into the following form.

$$\frac{C_T}{C_{T_\infty}} = \frac{Z/D}{[K_1 + K_2(C_{T_\infty}/\sigma)](Z/D) + [K_3 + K_4(C_{T_\infty}/\sigma)]} \tag{4.1}$$

This equation can be expressed in the form (4.2) in order to facilitate the calculation of the thrust coefficient at OGE corresponding to the C_T at IGE under the same power level:

$$C_T{}^* = \frac{[K_1(Z/D) + K_3]}{(1/C_T - K_2/\sigma)(Z/D) - K_4/\sigma} \tag{4.2}$$

7

The figure below illustrates the definition of $C_T{}^*$ as related to the C_T at IGE under constant C_P.
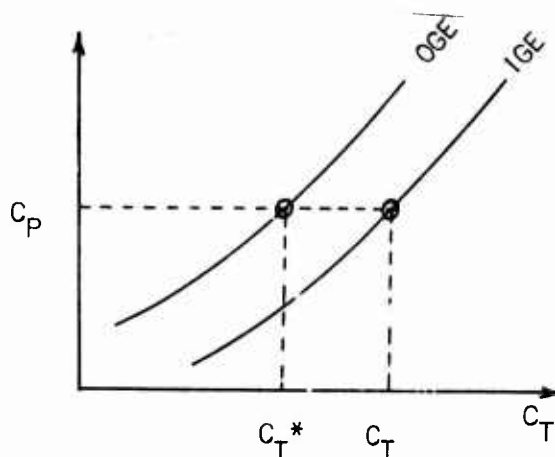
These are the two basic forms of the generalized hovering performance equation which will be employed for prediction. Equation (4.1) provides directly the relative thrust increase which is the main interest in hovering performance. However, equation (4.2) is useful in predicting C_T at an IGE value by first calculating the thrust coefficient $C_T{}^*$ corresponding to the C_T at that IGE skid height under constant C_P. Thus the point for that C_T and Z/D in question can be located.

The generalized equation (4.1) of hovering performance is plotted in Figure 17 with Z/D range from 0.2 to 1.4 and C_{T_∞}/σ range from 0.03 to 0.14. The method of prediction based on this generalized equation is very simple. First of all, the constants K_i, $i = 1,2,3,4$ can be obtained from flight data and are known. Then for a certain operating power level at a specified relative skid height Z/D, the relative thrust increase C_T/C_{T_∞} can be calculated readily. The various applications of this equation will be discussed in Section 3.7.

3.5 Flight Data Required for the Generalized Method of Prediction

This generalized method of prediction as presented in Section 3.4 requires only limited amount of flight data. This is one distinctive feature of this method of prediction. Furthermore, even with limited flight data, this prediction does not lose its accuracy within the limit of tolerance. The discussion on accuracy will be presented in Section 3.8. This feature allows the flight test engineer to reduce the amount and the range of flight test, therefore reducing the time, manhour and thus the cost of flight testing.

In this generalized method of prediction, the only required flight data of an aircraft is that of the OGE C_P - C_T data, or any one IGE skid height C_P - C_T data. From the available OGE data, IGE hovering performance at various skid heights can be predicted. Or for the case of available IGE data, the OGE and thus the rest of the IGE hovering performance can be predicted. Different applications using the generalized equations of prediction will be presented in Section 3.7. The figures below illustrate the

8

required flight data and the predicted performance:
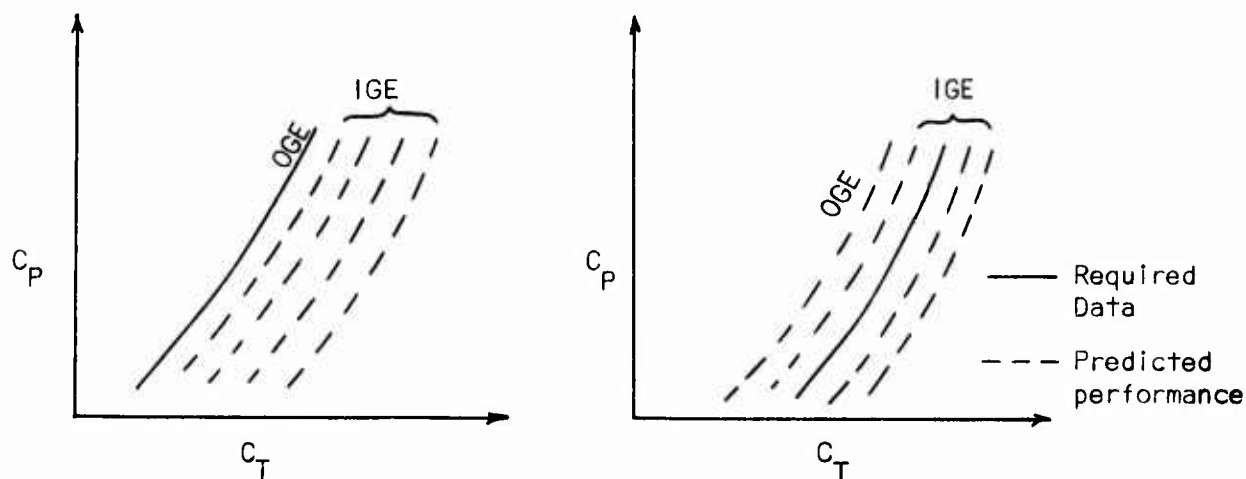
3.6 Suggested New Method of Flight Test: The Two-Point Method

From the functional relations of $(a, C_{T\infty}/\sigma)$ and $(b, C_{T\infty}/\sigma)$, it was observed that in each individual helicopter, the function relation of these two sets of parameters forms linear or very close to linear relationship as presented in Figures 15 and 16.

This phenomenon motivates a new method of flight test which not only will save time and reduce cost of testing as in the generalized method, but also provide better accuracy for hovering performance prediction. This accuracy will be compared with that of the generalized method. This new method suggests that, in addition to the information needed for the generalized method of prediction, helicopters be test flown at two constant power levels (C_P), one high and one low, at OGE and various IGE skid heights. The following figure shows the flight test data required.
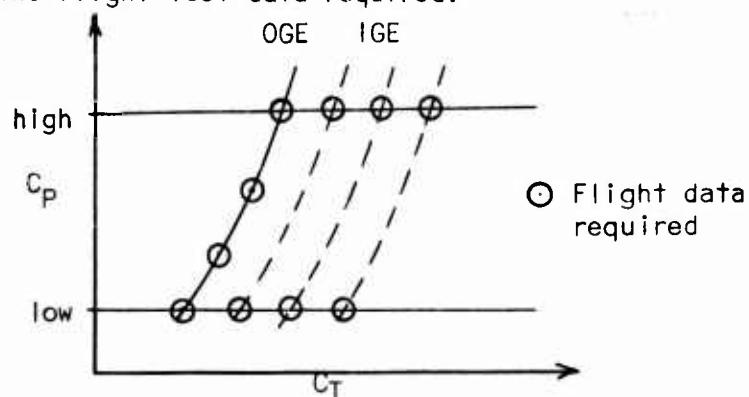
Then these data can be reduced to the parameters $C_T/C_{T\infty}$, Z/D, and $C_{T\infty}/\sigma$ as shown in the figure on the next page.

9
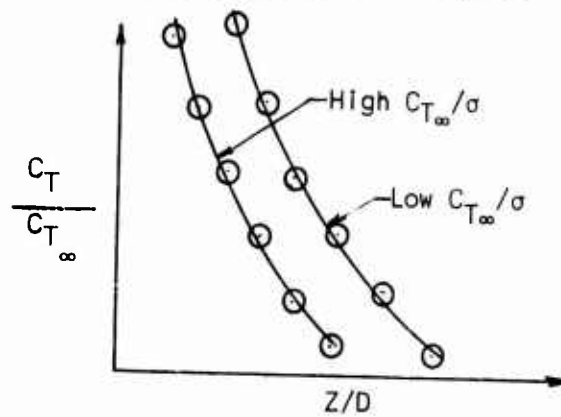
Each of the two curves is of the form $Y = \dfrac{X}{aX + b}$

The relation of a and b with $C_{T\infty}/\sigma$ can be represented in the figures below:

$$a = K_1 + K_2(C_{T\infty}/\sigma)$$

$$b = K_3 + K_4(C_{T\infty}/\sigma)$$

Having these two points and knowing that the intermediate points should follow a linear relationship very closely, a straight line is drawn through these two points, and a n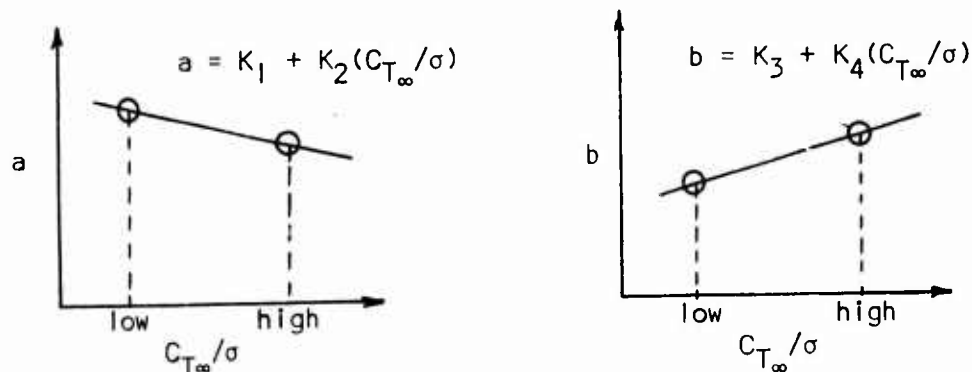ew set of values of the constant K's is obtained. With these new values, the generalized equation (4.1) can then be applied for the prediction of hovering performance. The accuracy of this Two-Point Method of prediction and the results of the test cases will be presented in Section 3.8.2.

This Two-Point Method of prediction provides better accuracy than the generalized method, and therefore serves as a substitute for the generalized method in the event that higher accuracy of prediction is needed. The only cost to this higher accuracy is the additional flight data at two power levels, one high and one low.

It is appropriate here to emphasize one requirement in using this method. Since the accuracy of this method depends heavily on the accuracy of flight test at the two power levels, it is, therefore, important that the data for these two points should be provided as accurately as possible.

3.7 Application

The aim of the application of these two methods of prediction is to facilitate a way to reduce flight test time so that with limited available

flight data, the entire range of flight testing can be accurately predicted. Thus, the cost of testing can be greatly reduced. In all cases, the aircraft characteristics should be available as compulsory input to this method of prediction. They include:

(1) skid to rotor hub height

(2) main rotor diameter

(3) main rotor solidity

The diversity of application of this method can be summarized into five categories:

(1) a. Prediction of relative thrust increase $(C_T/C_{T\infty})$, given only aircraft dimensional characteristics.

     b. Prediction of relative thrust increase $(C_T/C_{T\infty})$, given OGE.

(2) Prediction of IGE performance, given OGE flight data.

(3) Prediction of IGE performance, given predicted OGE performance by analytical formulation.

(4) Prediction of OGE and the rest of IGE performance, given one skid height IGE flight data.

(5) Prediction of IGE performance, given OGE and one low and one high power level flight data at various IGE. (Two-Point Method).

For detailed descriptions of applications, please refer to Section II of Appendix A.

3.8 Accuracy of Method

A method of this kind can be regarded as useful if its accuracy of prediction is within an acceptable tolerance and its application can facilitate the technical analysis resulting in the saving of time and cost. The methods presented in this report well meet these two criteria. Their accuracy is discussed in the following sections.

3.8.1 Accuracy of the Generalized Method

3.8.1.1 Comparison of the Predicted and Experimental Hovering Performance

One way to check the accuracy of this method is to simulate the hovering performance $(C_p - C_T$ relationship) of the helicopters and compare the result with the flight data. The aircraft YUH-ID (with 44 ft. rotor) was chosen as an example to demonstrate the accuracy of the generalized method of prediction. The accuracy of the prediction shows that in all cases of skid height, the

deviation from the flight data is less than 5%. A sample of this comparison is presented in Figure 18. In order to avoid cluttering the curves on one drawing, only skid heights of 2 and 10 ft. are shown in the figure. The prediction on the rest of the helicopters in this study shows an accuracy all within 5% deviation from the flight data.

3.8.1.2 Comparison of Relative Thrust Increase

To check the accuracy of prediction by comparing the predicted and the experimental relative thrust increase is of more immediate interest with respect to hovering performance. This comparison can be best realized by the presentation of a histogram showing the sample mean and standard deviation of this method of prediction. The histogram is presented in Figure 19. The distribution of deviation is of the normal form. The sample mean and standard deviation were computed to be -0.3642 and 2.0891 respectively. The following table shows a summary of this comparison.

Aircraft	Sample mean	Standard Deviation
All ten helicopters	-0.3642	2.0891

In other words, this comparison reveals that in the prediction of hovering performance considering all ten helicopters, about 68% of the predictions falls within the range of $\pm$ 2.0891% deviation from the flight data, and about 95% falls within the range of $\pm$ 4.1782% deviation for the flight data. The probability of prediction that will fall within a certain range of percentage deviation from the flight data is shown in Figure 20. It demonstrates clearly that in order to have an accuracy of prediction within the range of $\pm$ 5% deviation, which is an acceptable tolerance, this method of prediction is 98.98% successful.

3.8.1.3 Accuracy of Prediction on Helicopters Outside This Study

The next question to ask is whether this method of prediction can provide the same high degree of accuracy if applied to helicopters not included in this study. A satisfactory demonstration of this method of prediction on such helicopters will strengthen the confidence in this method.

Four helicopters with recent limited flight data (except for the case of YH-41 which was flight tested in 1960) were selected for this test case. They are OH-6A, LOH 206A, AH-1G and YH-41. In all these four cases, only the OGE and one IGE flight data were available (References 14 to 17). With the generalized equations (4.1) and (4.2), the hovering performance of all four helicopters was predicted and the $C_P - C_T$ curves generated. The

12

predicted performance and the flight data were then compared as shown in Figures 21 to 24. In all cases, the maximum deviations from the flight data based on the IGE skid height are less than 4.5%, and in particular for the cases of OH-6A and LOH 206A less than 2%. The relative thrust increase was also predicted and compared with the flight data as illustrated in Tables XII to XIII. It should be noted that since flight data of only one IGE skid height were available for each of the above helicopters, comparison of the relative thrust increase can only be based on that one IGE skid height. The results show that in all four helicopters and for the entire range of power level, the deviation of the predicted from the data is within 5%.

The accuracy of this method of prediction on all ten helicopters in this study and on four helicopters outside of this study not only demonstrates the usefulness and reliability in this method but also strengthens the confidence in using it.

In order to employ the Two-Point Method of prediction, flight data on two power levels and at various IGE skid heights should be available. At present, such data are not available, and therefore, this method cannot be readily used.

3.8.2 Accuracy of the Two-Point Method

In order to investigate the accuracy of this method, the hovering performance of all ten helicopters was predicted with this Two-Point Method. The results obtained were then compared with that of the generalized method and with the flight data. In all cases, the Two-Point Method provides closer prediction to the flight data than the generalized method. In order to demonstrate this comparison, the results on YUH-ID (48 ft. rotor) and the UH-IC were selected and are presented in Figures 25 and 26. In the figures only the skid heights of 2 and 10 ft. are shown for the sake of clarity. It can be observed clearly in the figures that the Two-Point Method indeed provides better accuracy than the Generalized Method.

This result of closer prediction is expected because of the fact that first of all the empirical functional relations of the constants a and b with respect to C_{T_∞}/σ on each helicopter are linear or very close to linear which can be seen in Figures 15 and 16. Secondly, these functional relations employed in this Two-Point Method are actually closer to the flight data than those employed in the generalized method.

4. CONCLUSIONS

In this report, two methods of prediction on helicopter hovering performance have been presented. The outstanding features of these methods are that first of all they are simple and easy to apply. Secondly, only limited flight data are required (OGE $C_P - C_T$ or IGE skid height $C_P - C_T$ data) for predictions on the entire range of hovering performance. Thirdly,

13

these simple methods provide highly accurate predictions. In all cases tested, the accuracy is well within 5% deviation from the flight data.

4.1 Prediction Methods

These two methods, the Generalized and the Two-Point Methods, employ the prediction equation derived empirically from a wide range of flight data. The derivation of this equation is presented in Section 2. The Two-Point Method is a more specific one which provides higher accuracy of prediction than the generalized one.

4.1.1 Generalized Method

This method uses the generalized prediction equation

$$\frac{C_T}{C_{T_\infty}} = \frac{Z/D}{[K_1 + K_2(C_{T_\infty}/\sigma)](Z/D) + [K_3 + K_4(C_{T_\infty}/\sigma)]}$$

The constants K_1, K_2, K_3, K_4 are pre-determined from the flight data considered in this study. The only flight data necessary for the prediction of the entire range of power level is the OGE or one IGE skid height $C_P - C_T$ performance. Once the required values of C_{T_∞}/σ and Z/D at which the hovering performance is to be predicted are given, the relative thrust increase C_T/C_{T_∞} can be readily calculated.

4.1.2 Two-Point Method

This method makes use of the linear relationship between a, b and C_{T_∞}/σ. The constants K_1, K_2, K_3, K_4 are determined for the particular helicopter in question by use of this linear relationship. Then the generalized prediction equation (4.1) is applied for the hovering performance calculation. This method requires, in addition to the OGE $C_P - C_T$ data, the $C_P - C_T$ flight data on two power levels, one high and one low, at various IGE skid heights. This Two-Point Method provides more accurate prediction than the Generalized Method.

4.2 Applications

These methods can be applied in different ways according to different given information as follows:

(I) a. Prediction of relative thrust increase (C_T/C_{T_∞}), given only aircraft dimensional characteristics.

     b. Prediction of relative thrust increase (C_T/C_{T_∞}), given OGE flight data.

14

(2) Prediction of IGE performance, given OGE flight data.

(3) Prediction of IGE performance, given predicted OGE performance by analytical formulation.

(4) Prediction of OGE and the rest of IGE performance, given one skid height IGE flight data.

(5) Prediction of IGE performance, given OGE and one low and one high power level flight data at various IGE. (Two-Point Method).

4.3 Suggested Data Information and Flight Test Method

Since the generalized method provides accurate prediction on hovering performance and requires limited flight data, it is suggested that the range of flight testing can be reduced to only the OGE C_P - C_T data or one IGE skid height C_P - C_T data. Hence, tremendous saving on time and manhour and therefore the cost of testing can be realized.

Should situation require that highly accurate prediction be needed, the Two-Point Method may then be employed. Since this method of prediction as indicated before requires the addition of C_P - C_T data at two power levels, a new method of flight testing is suggested in which the aircraft is to be test flown, in addition to the OGE range, at two constant power levels at various IGE skid heights.

4.4 Extension of These Methods of Prediction

The flight data available for this study have been limited mostly to single-rotor helicopters. However, the principles of these methods are applicable to the tandem types. These same methods of prediction can be employed upon the availability of sufficient flight data on tandem helicopters. Furthermore, if the interest of prediction on helicopter performance is confined to a certain type of helicopters, then a different set of values of the constants K_1, K_2, K_3, K_4 can be obtained based on a range of flight data of the type of helicopters in question, and the same methods can be applied.

These two simple methods of prediction on hovering performance are valuable tools in the aid of preliminary design, in accurate prediction of such performances, and in economizing flight testing. The results of prediction on ten helicopters and an additional four outside of this study show an accuracy within 5% deviation from flight data. Therefore, there is good confidence in the use of these methods.

15

APPENDIX A

APPLICATIONS, PROCEDURES AND SAMPLE CALCULATION OF METHOD OF PREDICTION

    This section is intended for those who are mainly interested in the working of the methods of prediction presented in this report. Description of applications, procedures, and sample calculations of these methods is the major objective in this Appendix.

I. GENERAL INFORMATION

I. Equations of Hovering Performance

    This method of prediction uses the generalized equation on hovering performance.

$$\frac{C_T}{C_{T_\infty}} = \frac{Z/D}{[K_1 + K_2(C_{T_\infty}/\sigma)](Z/D) + [K_3 + K_4(C_{T_\infty}/\sigma)]} \tag{A.1}$$

which can be expressed in the form of

$$C_T^* = \frac{[K_1(Z/D) + K_3]}{[1/C_T - K_2/\sigma](Z/D) - K_4/\sigma} \tag{A.2}$$

where C_T = Thrust coefficient at IGE
$\quad\quad C_T^*$ = Thrust coefficient at OGE corresponding to the same power level for a selected C_T at IGE.
$\quad\quad C_{T_\infty}$ = Thrust coefficient at OGE
$\quad\quad Z$ = Distance from ground to rotor hub (FT)
$\quad\quad D$ = Main rotor diameter (FT)
$\quad\quad \sigma$ = Main rotor solidity
$\quad\quad K's$ = Constants

2. The Constants

    In the above equations (A.1) and (A.2), the constants K_1, K_2, K_3, and K_4 have been previously determined. They are shown below:

$$K_1 = 1.099107$$
$$K_2 = -0.289447$$
$$K_3 = -0.104183$$
$$K_4 = 0.391297$$

These four constants will be changed if the Two-Point Method is applied on individual helicopters. Those who are interested in the calculation of these constants can refer to Section 3.6.

3. Aircraft Dimensional Characteristics

The following are the required characteristics of a helicopter as inputs to this method:

(1) Skid to rotor hub height (FT)

(2) Main rotor diameter (FT)

(3) Main rotor solidity

4. Inputs to Method of Prediction

Besides the aircraft dimensional characteristics which are necessary as inputs to these methods, the user of these methods should also decide at what skid heights and within what range of C_T should the hovering performance be predicted. Furthermore, the flight data on OGE or on one IGE skid height should also be available as given conditions which will be described in the following paragraphs.

In summary, the following items are the inputs:

Necessary Inputs

(1) Aircraft characteristics: (a) skid to rotor hub height (FT)

      (b) main rotor diameter (FT)

      (c) main rotor solidity

(2) Skid heights (FT)

(3) Range of C_T

(4) Values of constants K's

Variable Inputs

(1) Flight data ($C_P - C_T$ relationship) on OGE or on one IGE skid height

(2)   Flight data of OGE and various IGE under one high
      and one low power level (Two-Point Method)

(3)   Values of constants K's for individual aircraft
      (Two-Point Method)

II.   APPLICATIONS AND PROCEDURES

These methods of prediction can be applied in many ways depending on
what is to be predicted under what given conditions. In general, there
are five ways in which these methods are applicable:

(1) a.   Prediction of relative thrust increase ($C_T/C_{T\infty}$), given only
          aircraft dimensional characteristics.

     b.   Prediction of relative thrust increase ($C_T/C_{T\infty}$), given OGE.

(2) Prediction of IGE performance, given OGE flight data.

(3) Prediction of IGE performance, given predicted OGE performance
     by analytical formulation.

(4) Prediction of OGE and the rest of IGE performance, given one
     skid height IGE flight data.

(5) Prediction of IGE performance, given OGE and one low and one
     high power level flight data at various IGE. (Two-Point Method).

These five applications are individually discussed and described below.

1.1   Application (1a): Prediction of Relative Thrust Increase, Given Only
Aircraft Dimensional Characteristics

This is the most general and overall way of predicting the relative thrust
increase. The chart below shows the inputs and output of this prediction:

Input	Output
1. Aircraft dimensional characteristics	1. Relative thrust
2. Skid heights in terms of Z/D	increase C_T/C_{T_∞}
3. Range of power levels, $C_{T\infty}/\sigma$	

18

Equation (A.1) can be directl/ applied, and the relative thrust increase can be readily calculated.

Procedures

(1) Pick various skid heights to calculate the corresponding Z/D

(2) Pick a range of $C_{T\infty}/\sigma$

(3) Apply equation (A.1) to obtain $C_T/C_{T\infty}$

This application only provides a general perspective on hovering performance because of the fact that the values of $C_{T\infty}/\sigma$ selected may not be that for the real situation.

1.2 Application (Ib): Prediction of $C_T/C_{T\infty}/\sigma$, given OGE

The only difference between this application and that of (Ia) as far as input information is concerned is that the OGE $C_P - C_T$ relation is available from which $C_{T\infty}/\sigma$ can be obtained corresponding to the real situation.

The following chart shows the inputs and the output of this prediction.

Input	Output
1. Aircraft dimensional characteristics	1. $C_T/C_{T\infty}$
2. Skid heights in terms of Z/D	
3. OGE $C_P - C_T$ data	

Again equation (A.1) can be applied directly. The following are the procedures:

(1) Pick a range of Z/D

(2) Pick values of $C_{T\infty}/\sigma$ for the real situation

(3) Apply equation (A.1) to obtain corresponding $C_T/C_{T\infty}$

1.3 Application (2): Prediction of IGE, given OGE

In this application, once the OGE $C_P - C_T$ flight data are given, all IGE $C_P - C_T$ relations can be predicted. To do so, the generalized equations (A.1) and (A.2) are applied. The approach is disgrammed in the following figure.
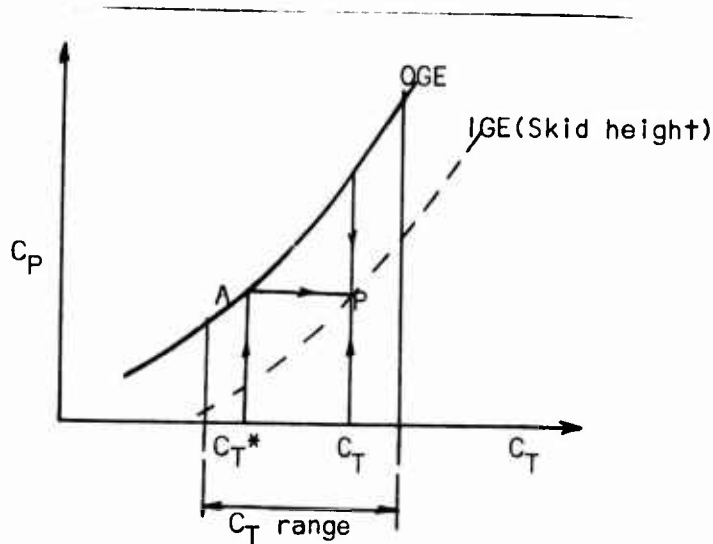
Let r be any point within the C_T range to be predicted for a certain in-ground Z/D. The procedures are as follows:
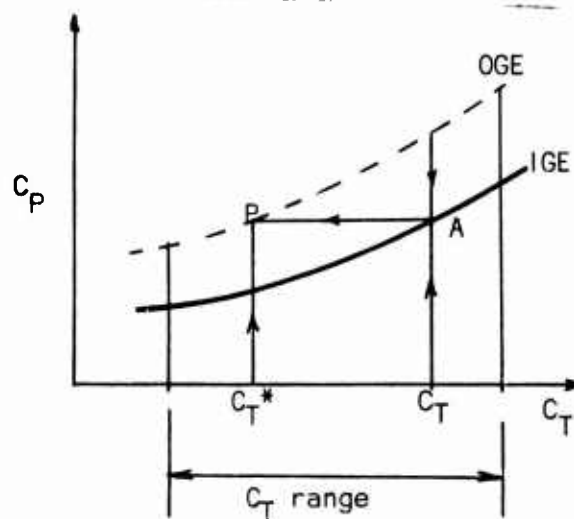
(1) Pick a C_T within the range, and a skid height.

(2) Calculate C_T^* from equation (A.2).

(3) Draw a vertical line through the value of C_T^*, intersecting OGE at point A, and draw a vertical line through the value of C_T.

(4) Draw constant C_P line through A on OGE.

(5) The intersection P of this constant C_T and C_P lines is the point to be predicted for this selected IGE.

(6) Pick another C_T value and repeat steps (1) to (5). Eventually the entire C_P - C_T relation for this skid height can be predicted.

(7) Pick another skid height and repeat the same process from steps (1) to (6) to predict the C_P - C_T curve for this new skid height.

1.4 Application (3): Prediction of IGE, given predicted OGE.

This application follows exactly the same procedures as that of Application (2), except that the additional error source is from the analytical formulation of OGE.

1.5 Application (4): Prediction of OGE and IGE, given one IGE

This method of prediction is similar to that of the Application (2) except the logic is reversed. The following figure demonstrates this procedure.

20

Procedures

(1) Pick a C_T within the range.

(2) Calculate C_T^* from equation (A.2)

(3) Draw a vertical C_T line, intersecting the IGE at A.

(4) Draw a vertical C_T^* line and a constant C_P line through A.

(5) The intersection P of the constant C_P and C_T lines is the point to be predicted at OGE.

(6) Pick another C_T value, repeat steps (1) to (5), to predict the entire OGE.

(7) With this OGE, predict the rest of the IGE by the same procedure as in Application (2).

1.6 Application (5): Prediction of IGE, Given Two Power Level Data and OGE

This application ties in with the Two-Point Method of flight test which will provide a closer prediction. In addition to OGE flight data, it is required to obtain data at two constant power levels, one high and one low at various IGE skid heights. After the constants K_1, K_2, K_3, K_4, are obtained, which was discussed in Section 3.6, the hovering performance can be predicted with these new values of K's by following the same procedures as in Application (2) to (4) with respect to the corresponding given conditions.

The following is a summary of the applications of the method of prediction.

21

Application	To Be Predicted	Given Conditions	Special Conditions
1a	C_T/C_{T_∞}	Aircraft Dimensional Characteristics Only	None
1b	C_T/C_{T_∞}	OGE	None
2	IGE	OGE	None
3	IGE	Predicted OGE	None
4	OGE, IGE	One IGE	None
5	IGE	OGE	IGE flight data at one high and one low power level C_P

III. SAMPLE CALCULATIONS

There are five different applications of this method of prediction. Because of the similarity of procedures, only two typical applications are presented here as sample calculations. They are

(A) Application (2): Prediction of IGE, given OGE

(B) Application (5): Prediction of IGE, by the Two-Point Method

The aircraft UH-IC is employed here as an example.

Application (2)

In this application, the OGE C_P - C_T data are provided.

Input Information:

Necessary inputs:

1. Aircraft characteristics: (a) Skid to rotor hub height = 12.26 ft.

   (b) Main rotor diameter = 44 ft.

   (c) Main rotor solidity = 0.0651

2. Skid heights 2, 5, 10, 15, 25, 50 (OGE) ft.

3. Range of C_T: 35×10^4 to 60×10^4

4. $K_1 = 1.099107$
   $K_2 = -0.289447$
   $K_3 = -0.104183$
   $K_4 = 0.391397$

Variable inputs:

1. OGE $C_P - C_T$ data

Procedures:

1. Pick the values of C_T to be 35, 40, 45, 50, 55, 60, $\times 10^4$ and the skid heights of 2, 5, 10, 15, 25, 50 ft.

2. Calculate C_T^* with equation (A.2) with the above values of C_T and Z/D The calculated values of C_T^* and their corresponding values of C_T and Z/D are listed on Table A-1.

3. Plot the OGE $C_P - C_T$ data in Figure A.1.

4. Locate all the in-ground C_T points with respect to the OGE curve by following the procedures (3) to (7). The result is presented in Figure A.1.

Application (5)

Input Information

The input information is the same as that of the previous sample calculations, except for the constants K's. These constants are obtained from the linear functions of $(a, C_{T_\infty}/\sigma)$ and $(b, C_{T_\infty}/\sigma)$.

The values of "a" and "b" corresponding to the high and low power levels are as follows:

Values	High Power Level	Low Power Level
C_{T_∞}/σ	0.076344	0.054378
a	1.083304	1.105835
b	-.079061	-0.091799

The linear equations of $(a, C_{T_\infty}/\sigma)$ and $(b, C_{T_\infty}/\sigma)$ can be obtained as

$$a = 1.161612 - 1.025722 (C_{T_\infty}/\sigma)$$
$$b = -.0123333 + 0.5799 (C_{T_\infty}/\sigma)$$

23

Therefore the values of K's are:

$$K_1 = 1.161612$$
$$K_2 = -1.025722$$
$$K_3 = -0.123333$$
$$K_4 = 0.5799$$

With these values of K's, follow the same procedures of calculation as in the previous case. The values of C_T^* are listed on Table A-11, and the predicted performance is presented in Figure A.2.

APPENDIX B

SUITABILITY OF THE EMPIRICAL FUNCTIONS

To simulate the flight test data, a number of empirical functions were selected. The objective is to establish whether or not the function truly represents the experimental information. One way to determine the suitability of these functions is the linear graphical test.

In this test, the hypothesized function $F(x, y)$ was rewritten in a linear form with respect to two selected functions f_1 and f_2:

$$f_1 = n + mf_2$$

where m, n are constants

in the case of the power function, the linear form is

$$\log y = a + (b) \log y$$

and in the case of the first and second hyperbolic functions, the linear forms are respectively

$$xy = ax + b$$

$$\text{and} \quad x/y = ax + b$$

$$\text{where} \quad x = Z/D, \text{ and } y = C_T/C_{T_\infty}$$

Then the pairs of data values of x and y were substituted into the linear equation $f_1 = n + mf_2$, and f_1 was plotted as a function of f_2. As long as a straight line is obtained from this test, we can consider this result as an indication that the hypothesized equation may be satisfactory.

The linear graphical test of these three functions were plotted in Figure B-1. It can be readily observed that the second hyperbolic function leads to the closest linear relation between f_1 and f_2. The actual plot of these three functions against the flight data for the case of YHU-1B is presented in Figure 12. It is clear from the figure that the second hyperbolic function is the best choice.

25

REFERENCES

1. Knight, M: and Hefner, R.A.: "Analysis of Ground Effect on the Lifting Airscrew." NACA TN835, 1941.

2. Zbrozek, J.: "Ground Effect on the Lifting Rotor." British ARC R&M No. 2347, July, 1947.

3. Gessow, A; and Myers, G.C. Jr.: "Aerodynamics of the Helicopter." Frederich Ungar Publishing Co. Inc., New York, 1967.

4. Ralston, A.: "A First Course in Numerical Analysis." McGraw - Hill Book Company, New York, 1965.

5. Porter, D.W.; and Flanagen, E.G.: "Category II Performance Tests of the YUH-ID with a 48-Foot Rotor." USAF FTC-TDR-64-27.

6. MacPherson, D.F. Jr.; and Hodgson, W.J.: "ARDC YH-40 Performance Evaluation.: AFFTC-TR-59-33, January, 1960.

7. Johns, S.L.; and Colvin, G.L.: "YHU-IB Category II Performance Tests." FTC-TDR-62-21, December 1962.

8. Reschak, R.J.; and Balwin, R.L.: "YUH-ID (44-Foot Rotor) Category II Performance." TDC-TDR-63=43, November, 1964.

9. Smith, E.J.; and Kidwell, J.C.: "Limited Evaluation of the Bell Model 47 J-2." ATO-TR-62-5, May, 1962.

10. Kidwell, J.: and Johnston, J.A." "Evaluation of the Hiller Model UH-12E-4 Helicopter." ATO-TR-62-7.

11. Schroers, L.G.; and Melton, J.R.: "Engineering Flight Test of the UH-IB Helicopter equipped with the Model 540 Rotor System. Phase D Final Report." AD 811782, USATECOM Project No. 4-4-0108-03, December 1966.

12. Tanaka, F.H.; Blafe, J.J.; and Somsel, J.R.: "Category II Performance Tests of the CH-47A Helicopter." FTC-TR-66-2, May, 1966.

13. Ferrel, K.R.; and Ferry, R.G.: "ARDC YHO-2HU Air Force Flight Evaluation." AFFTC-TR-60-2, February 1960.

14. Koelle, E.A.; and Hodgson, W.J.: "ARDC YH-41 Performance Evaluation." AFFTC-TR-60-7, May 1960.

15. "Detailed Specification Light Observation Helicopter LOH 206A" Revision No. R-3, January 15, 1968, Bell Helicopter.

16. Crouch, W.E., Jr. E.P. Preisendorfer, K.R. Ferrell, "Engineering
     Flight Test of the Light Observation Helicopter (LOH) OH-6A Armed
     (XM-27E1) and Unarmed Performance and Stability and Control," USAAVCOM
     Project No. 67-13, December 1967.

17. Private Correspondence on AH-1G.

SYMBOLS

C_P Rotor-shaft power coefficient

C_T Thrust coefficient

C_{T_∞} Thrust coefficient at OGE under the same power level

C_T^* Thrust coefficient at OGE corresponding to C_T at IGE for the same C_P

D   Rotor diameter (FT)

IGE   In-ground-effect

OGE   Out-of-ground effect

Z   Ground to rotor hub height

σ Rotor solidity

TABLE I

AIRCRAFT DIMENSIONAL CHARACTERISTICS

Aircraft	Skid to Rotor Distance, Ft.	Solidity	Rotor Diameter Feet
Single - rotor			
47 J-2 (Bell)	10.12	.0316	37.125
UH-12E-4	10.125	.0343	35.333
YH-40	11.0	.0362	44
YHO-2HU	7.917	.0430	25
YUH-1D	11.96	.0464	48
YUH-1D	11.96	.0506	44
YUH-1B	12.4	.0506	44
UH-1C (540 rotor)	12.26	.0651	44
CH-54A	18.583	.1021	72
Tandem			
CH-47A	18.583(1)	.0620	59.104

(1) to rear rotor

Table II YUH-1D Test Data

$C_P \times 10^5$	$C_{T\infty}/\sigma$	Skid Ht	60 (OGE)	40	30	20	15	10	5	2
		z/D	1.5	1.082	0.874	0.665	0.561	0.4575	0.353	0.291
20	.0583	$C_T \times 10^4$	27.1	27.1	27.2	27.6	27.9	28.7	30.0	32.0
		$C_T / C_{T\infty}$	1.0	1.0	1.002	1.018	1.03	1.06	1.106	1.18
22	.0634	$C_T \times 10^4$	29.4	29.4	29.45	29.9	30.3	31.1	32.5	34.7
		$C_T / C_{T\infty}$	1.0	1.0	1.002	1.018	1.03	1.058	1.106	1.18
24	.0678	$C_T \times 10^4$	31.5	31.5	31.6	32.2	32.6	33.5	35.0	37.2
		$C_T / C_{T\infty}$	1.0	1.0	1.002	1.022	1.035	1.064	1.112	1.181
26	.0724	$C_T \times 10^4$	33.6	33.6	33.6	34.3	34.7	35.7	37.4	39.6
		$C_T / C_{T\infty}$	1.0	1.0	1.0	1.02	1.032	1.062	1.112	1.178
28	.0765	$C_T \times 10^4$	35.5	35.5	35.5	36.2	36.8	37.8	39.7	42.0
		$C_T / C_{T\infty}$	1.0	1.0	1.0	1.018	1.035	1.065	1.118	1.182
30	.0803	$C_T \times 10^4$	37.3	37.3	37.5	38.2	38.8	39.8	41.8	44.2
		$C_T / C_{T\infty}$	1.0	1.0	1.005	1.022	1.04	1.066	1.12	1.183

Table III UH-1C Test Data

$c_p \times 10^5$	$c_{T\infty}/\sigma$	Skid Ht	50 (OGE)	25	15	10	5	2
		z/D	1.415	0.8468	0.6195	0.5059	0.3923	0.3241
30	.0544	$c_T \times 10^4$	35.4	36.0	36.9	37.9	40.1	43.5
		$c_T/c_{T\infty}$	1.0	1.0169	1.0424	1.0706	1.1328	1.2288
32	.0576	$c_T \times 10^4$	37.5	38.1	39.0	40.1	42.5	45.7
		$c_T / c_{T\infty}$	1.0	1.016	1.040	1.0693	1.133	1.2187
34	.0607	$c_T \times 10^4$	39.5	40.1	41.1	42.2	44.9	47.9
		$c_T / c_{T\infty}$	1.0	1.0152	1.0405	1.0684	1.1367	1.2127
36	.0636	$c_T \times 10^4$	41.4	42.1	43.1	44.3	47.2	50.0
		$c_T / c_{T\infty}$	1.0	1.0169	1.0411	1.0700	1.1401	1.2077
38	.0664	$c_T \times 10^4$	43.2	43.9	45.0	46.35	49.3	51.9
		$c_T / c_{T\infty}$	1.0	1.0162	1.0417	1.0729	1.1412	1.2014
40	.0691	$c_T \times 10^4$	45.0	45.65	46.9	48.3	51.3	53.8
		$c_T / c_{T\infty}$	1.0	1.0144	1.0422	1.0733	1.1400	1.1956
42	.0716	$c_T \times 10^4$	46.6	47.3	48.6	50.1	53.2	55.7
		$c_T / c_{T\infty}$	1.0	1.0150	1.0429	1.0751	1.1416	1.1953
44	.0740	$c_T \times 10^4$	48.2	49.0	50.2	51.7	54.9	57.5
		$c_T / c_{T\infty}$	1.0	1.0166	1.0415	1.0726	1.1390	1.1930
46	.0763	$c_T \times 10^4$	49.7	50.55	51.7	53.4	56.5	59.25
		$c_T / c_{T\infty}$	1.0	1.0171	1.0402	1.0745	1.1368	1.1922

Table IV CH-54A Test Data

$C_P \times 10^5$	$C_{T\omega}/\sigma$	Skid Ht	100 (OGE)	50	40	20	10	5
		z/D	1.65	0.953	0.815	0.535	0.396	0.327
40	.0447	$C_T \times 10^4$	45.7	46.5	47.5	50.3	53.5	55.9
		$C_T / C_{T\omega}$	1.0	1.018	1.04	1.10	1.171	1.225
50	.0546	$C_T \times 10^4$	55.8	56.7	57.7	60.8	64.7	67.3
		$C_T / C_{T\omega}$	1.0	1.015	1.033	1.09	1.158	1.205
60	.0635	$C_T \times 10^4$	64.8	65.5	66.7	70.0	74.2	77.2
		$C_T / C_{T\omega}$	1.0	1.01	1.028	1.079	1.143	1.19
70	.0712	$C_T \times 10^4$	72.7	73.7	75.0	78.7	82.9	86.6
		$C_T / C_{T\omega}$	1.0	1.014	1.032	1.082	1.14	1.192

Table V   CH-47A Test Data

$C_P \times 10^5$	$C_{T\infty}/\sigma$	Skid Ht	100 (OGE)	60	40	20	10	5
		Z/D	2.01	1.33	0.992	0.654	0.484	0.40
32	.0626	$C_T \times 10^4$	38.8	39.0	39.8	42.5	44.7	46.3
		$C_T / C_{T\infty}$	1.0	1.005	1.025	1.095	1.152	1.195
36	.0692	$C_T \times 10^4$	42.8	43.0	43.9	46.5	48.75	50.4
		$C_T / C_{T\infty}$	1.0	1.004	1.025	1.085	1.138	1.175
40	.0748	$C_T \times 10^4$	46.3	46.4	47.5	50.0	52.5	54.1
		$C_T / C_{T\infty}$	1.0	1.001	1.025	1.08	1.132	1.168
44	.0795	$C_T \times 10^4$	49.3	49.6	50.7	53.5	55.9	57.5
		$C_T / C_{T\infty}$	1.0	1.005	1.028	1.085	1.132	1.165

33

Table VI   YH-40 Test Data

$C_P \times 10^5$	$C_{T\infty}/\sigma$	Skid Ht	51.8 (OGE)	26.8	21.8	16.8	11.8	6.8	1.8
		Z/D	1.416	0.848	0.734	0.620	0.507	0.393	0.280
20	.0737	$C_T \times 10^4$	26.7	26.7	26.8	27.0	27.7	28.9	31.8
		$C_T / C_{T\infty}$	1.0	1.0	1.002	1.01	1.036	1.081	1.19
24	.0856	$C_T \times 10^4$	31.0	31.0	31.1	31.4	32.1	33.7	37.1
		$C_T / C_{T\infty}$	1.0	1.0	1.002	1.012	1.035	1.086	1.196
28	.0970	$C_T \times 10^4$	35.1	35.1	35.25	35.6	36.4	38.2	41.8
		$C_T / C_{T\infty}$	1.0	1.0	1.004	1.015	1.037	1.09	1.192
32	.1077	$C_T \times 10^4$	39.1	39.1	39.2	39.6	40.4	42.3	45.7
		$C_T / C_{T\infty}$	1.0	1.002	1.005	1.015	1.036	1.085	1.172
36	.1182	$C_T \times 10^4$	42.8	42.85	42.9	43.2	44.1	45.8	48.9
		$C_T / C_{T\infty}$	1.0	1.001	1.002	1.01	1.03	1.07	1.14
40	.1275	$C_T \times 10^4$	46.2	46.2	46.4	46.6	47.3	49.1	51.5
		$C_T / C_{T\infty}$	1.0	1.0	1.004	1.01	1.025	1.062	1.115

Table VII   YUH-1B Test Data

$C_P \times 10^5$	$C_{T\infty}/\sigma$	Skid Ht	45 (OGE)	35	25	15	10	5	1
		Z/D	1.305	1.077	0.850	0.622	0.509	0.395	0.305
30	.0722	$C_T \times 10^4$	36.5	36.5	36.7	38.0	39.1	41.1	44.0
		$C_T / C_{T\infty}$	1.0	1.0	1.005	1.04	1.07	1.126	1.205
32	.0763	$C_T \times 10^4$	38.6	38.7	38.9	40.1	41.2	43.3	46.3
		$C_T / C_{T\infty}$	1.0	1.002	1.008	1.04	1.067	1.12	1.2
34	.0802	$C_T \times 10^4$	40.6	40.6	40.9	42.1	43.2	45.4	48.4
		$C_T / C_{T\infty}$	1.0	1.0	1.009	1.04	1.065	1.12	1.192
38	.0873	$C_T \times 10^4$	44.2	44.3	44.6	45.8	47.0	49.2	52.2
		$C_T / C_{T\infty}$	1.0	1.002	1.01	1.035	1.063	1.112	1.18
40	.091	$C_T \times 10^4$	46.0	46.0	46.4	47.6	48.8	50.1	54.1
		$C_T / C_{T\infty}$	1.0	1.0	1.01	1.035	1.06	1.09	1.177
42	.094	$C_T \times 10^4$	47.6	47.7	48.0	49.3	50.6	52.9	55.9
		$C_T / C_{T\infty}$	1.0	1.001	1.01	1.037	1.063	1.11	1.175

Table VIII Bell 47 J-2

$C_P \times 10^5$	$C_{T\infty}/\sigma$	Skid Ht	40 (OGE)	20	10	5	2
		Z/D	1.35	0.81	0.542	0.408	0.327
14	.057	$C_T \times 10^4$	18.0	18.5	19.3	19.9	22.3
		$C_T / C_{T\infty}$	1.0	1.028	1.071	1.105	1.24
16	.0658	$C_T \times 10^4$	20.8	21.4	22.2	23.3	25.6
		$C_T / C_{T\infty}$	1.0	1.03	1.068	1.12	1.23
18	.07744	$C_T \times 10^4$	23.5	24.1	25.0	26.3	28.7
		$C_T / C_{T\infty}$	1.0	1.026	1.064	1.120	1.221
20	.082	$C_T \times 10^4$	25.9	26.7	27.6	28.9	31.6
		$C_T / C_{T\infty}$	1.0	1.03	1.065	1.115	1.22
22	.0892	$C_T \times 10^4$	28.2	29.0	30.0	31.4	34.2
		$C_T / C_{T\infty}$	1.0	1.028	1.063	1.113	1.212

Table IX UH 12E-4

$C_P \times 10^5$	$C_{T\infty}/\delta$	Skid Ht	50 (OGE)	20	10	5	2
		Z/D	1.7	0.852	0.57	0.428	0.344
18	.0708	$C_T \times 10^4$	24.3	24.6	25.3	26.3	27.6
		$C_T / C_{T\infty}$	1.0	1.012	1.04	1.082	1.135
20	.0782	$C_T \times 10^4$	26.85	27.1	27.95	29.0	30.45
		$C_T / C_{T\infty}$	1.0	1.009	1.041	1.080	1.134
22	.0853	$C_T \times 10^4$	29.25	29.55	30.45	31.6	33.15
		$C_T / C_{T\infty}$	1.0	1.01	1.04	1.08	1.132
24	.0921	$C_T \times 10^4$	31.6	31.9	32.9	34.1	35.8
		$C_T / C_{T\infty}$	1.0	1.01	1.04	1.08	1.132

Table X YHO-2HU Test Data

$C_p \times 10^5$	$C_{T\infty}/\sigma$	Skid Ht	33(OGE)	18	13	8	2.6
		z/D	1.6367	1.0367	0.8367	0.6367	0.4207
28	.0830	$C_T \times 10^4$	35.7	36.0	36.0	37.2	39.3
		$C_T \times C_{T\infty}$	1.0	1.0084	1.0084	1.0420	1.1008
32	.0921	$C_T \times 10^4$	39.6	39.8	39.8	41.1	43.65
		$C_T \times C_{T\infty}$	1.0	1.0051	1.0051	1.0379	1.1023
36	.1005	$C_T \times 10^4$	43.2	43.3	43.5	44.9	47.8
		$C_T \times C_{T\infty}$	1.0	1.0023	1.0069	1.0394	1.1065
40	.1086	$C_T \times 10^4$	46.7	46.7	47.1	48.55	51.8
		$C_T \times C_{T\infty}$	1.0	1.0	1.0086	1.0396	1.1092
44	.1165	$C_T \times 10^4$	50.1	50.1	50.6	52.1	55.5
		$C_T \times C_{T\infty}$	1.0	1.0	1.0100	1.0399	1.1078

Table XI YUH-1D (44 Foot Rotor) Test Data

$C_T \times 10^5$	C_{T_∞}/σ	Skid Ht	60 (OGE)	40	30	20	10	5	2
		z/D	1.64	1.18	0.95	0.73	0.50	0.39	0.32
30	.0716	$C_T \times 10^4$	36.25	36.25	36.25	37.1	39.0	40.9	42.55
		C_T / C_{T_∞}	1.0	1.0	1.0028	1.0235	1.0759	1.1283	1.1738
34	.0787	$C_T \times 10^4$	39.8	39.9	40.1	41.1	43.1	44.9	46.6
		C_T / C_{T_∞}	1.0	1.0025	1.0075	1.0327	1.0829	1.1281	1.1709
38	.0856	$C_T \times 10^4$	43.3	43.5	43.9	44.9	47.0	48.85	50.6
		C_T / C_{T_∞}	1.0	1.0046	1.0139	1.0370	1.0855	1.1282	1.1686
42	.0922	$C_T \times 10^4$	46.65	46.9	47.4	48.6	50.7	52.5	54.4
		C_T / C_{T_∞}	1.0	1.0054	1.0161	1.0418	1.0868	1.1254	1.1661
46	.0984	$C_T \times 10^4$	49.8	50.1	50.7	51.95	54.1	55.9	58.05
		C_T / C_{T_∞}	1.0	1.0060	1.0181	1.0432	1.0864	1.1225	1.1657
50	.1044	$C_T \times 10^4$	52.8	53.1	53.85	55.1	57.2	58.9	61.4
		C_T / C_{T_∞}	1.0	1.0057	1.0199	1.0436	1.0833	1.1155	1.1629

TABLE XII

PREDICTED RELATIVE THRUST INCREASE

BY THE GENERALIZED METHOD

Aircraft	$C_P \times 10^5$	C_T/σ	Z/D	$(C_T/C_{T_\infty})_D$	$(C_T/C_{T_\infty})_C$	γ
OH-6A	30	0.0684	0.4444	1.1183	1.1049	1.213
	32	0.0730		1.1058	1.1016	0.381
	34	0.0770		1.0979	1.0987	-0.073
	36	0.0807		1.0957	1.0960	-0.027
	38	0.0841		1.0941	1.0937	0.037
	40	0.0873		1.0905	1.0914	-0.082
	42	0.0904		1.0894	1.0892	0.018
	44	0.0934		1.0866	1.0871	-0.046
	46	0.0963		1.0859	1.0851	0.074
LOH 206A	18	0.0614	0.4067	1.1146	1.1309	-1.441
	20	0.0675		1.1151	1.1257	-0.942
	22	0.0731		1.1163	1.1210	-0.419
	24	0.0782		1.1242	1.1167	0.672
	26	0.0830		1.1287	1.1126	1.447

$(C_T/C_{T_\infty})_D$ = flight data

$(C_T/C_{T_\infty})_C$ = predicted values

$$\gamma = \frac{(C_T/C_{T_\infty})_D - (C_T/C_{T_\infty})_C}{(C_T/C_{T_\infty})_C}$$

40

TABLE XIII

PREDICTED RELATIVE THRUST INCREASE

BY THE GENERALIZED METHOD

Aircraft	$Cp \times 10^5$	C_{T_∞}/σ	Z/D	$(C_T/C_{T_\infty})_D$	$(C_T/C_{T_\infty})_C$	γ
AH-1G	26	0.0552	0.3086	1.175	1.2261	-4.168
	30	0.0624		1.1671	1.2156	-3.990
	34	0.0686		1.1723	1.2068	2.859
	38	0.0744		1.1753	1.1985	-1.936
	42	0.0802		1.1740	1.1904	-1.378
YH-41	18	0.0801	0.326	1.1494	1.1733	-2.037
	20	0.0873		1.1245	1.1643	-3.418
	22	0.0940		1.1093	1.1561	-4.048
	24	0.1006		1.0975	1.1481	-4.407
	26	0.1067		1.0920	1.1407	-4.269
	28	0.1124		1.0904	1.1340	-3.759

Figure 1

EMPIRICAL EFFECT OF ROTOR HEIGHT ON

ROTOR THRUST AT CONSTANT POWER

T = Rotor thrust within ground effect
T_∞ = Rotor thrust at OGE

$c_{T_\infty}/\sigma = 1.4 \times 0.025$

0.05 x 1.4
0.10 x 1.4
0.15 x 1.4
0.20 x 1.4
0.25 x 1.4

T/T_∞

Z/D
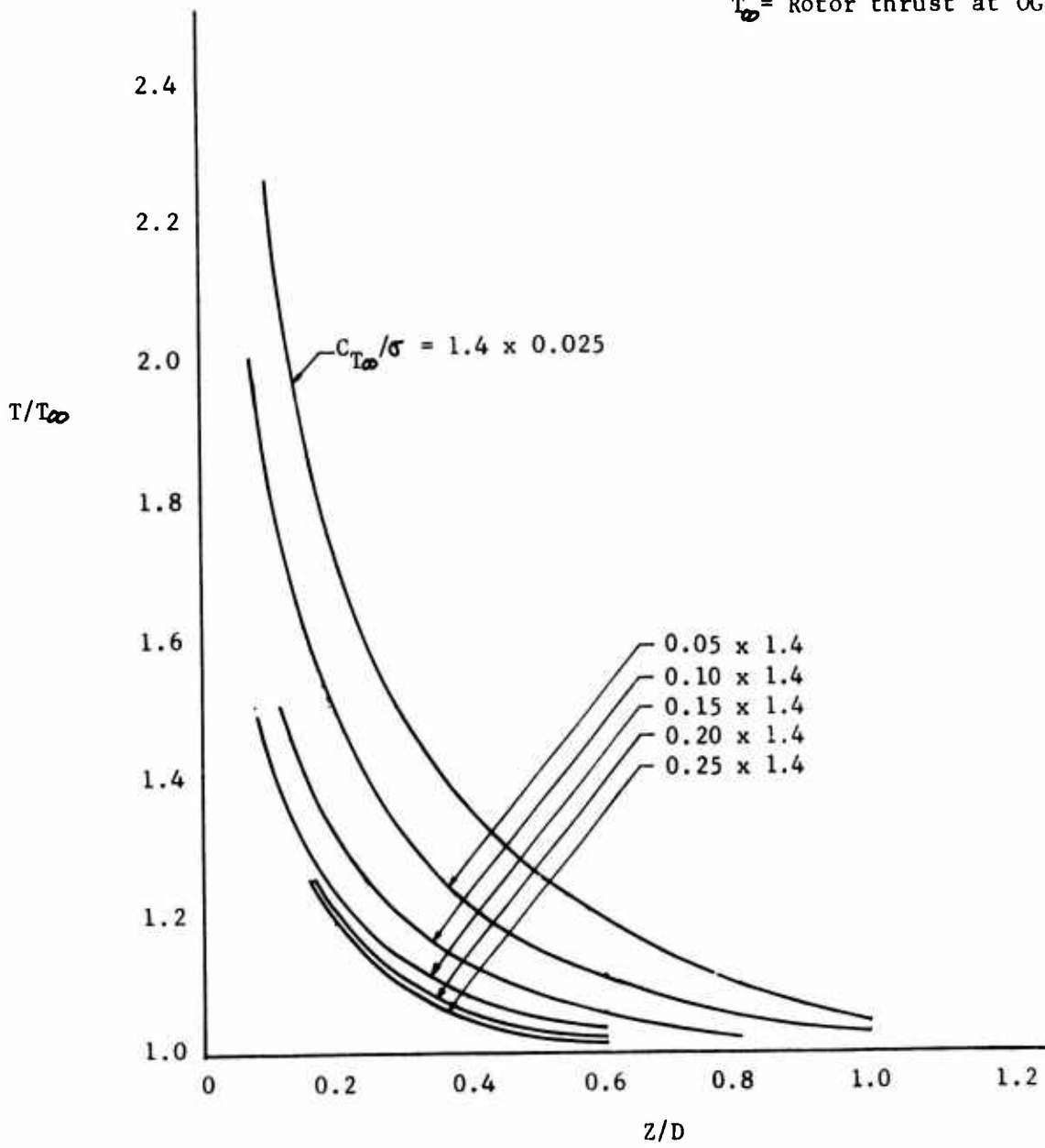
Figure 2

FLIGHT TEST DATA

Bell 47 J-2

$C_T/C_{T\infty}$ versus Z/D

Legend:

Symbol	$C_{T\infty}/\sigma$
⊙	0.0570
☐	0.0658
◇	0.0744
△	0.0820
◁	0.0892
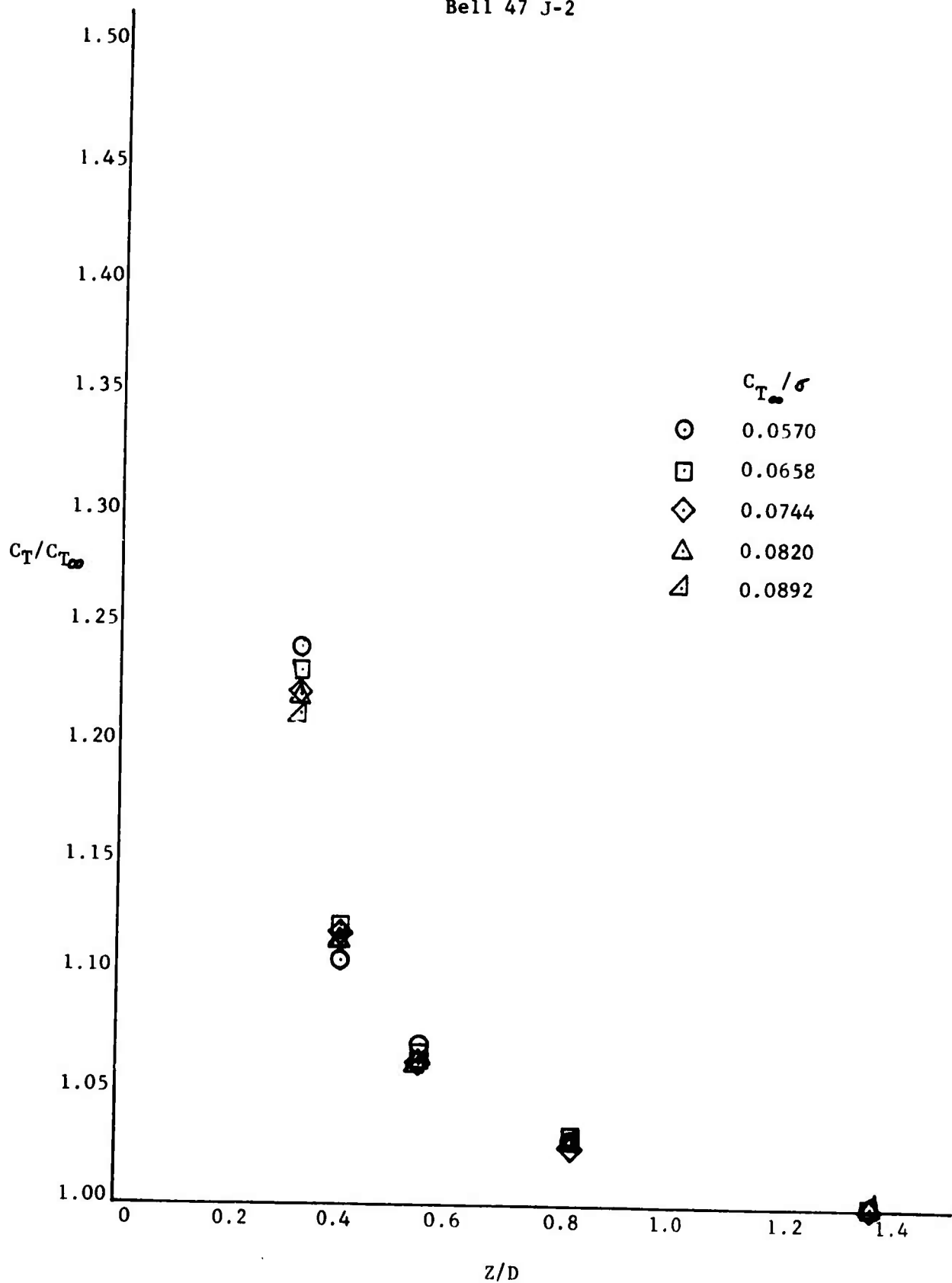
Figure 3

FLIGHT TEST DATA

UH 12E-4
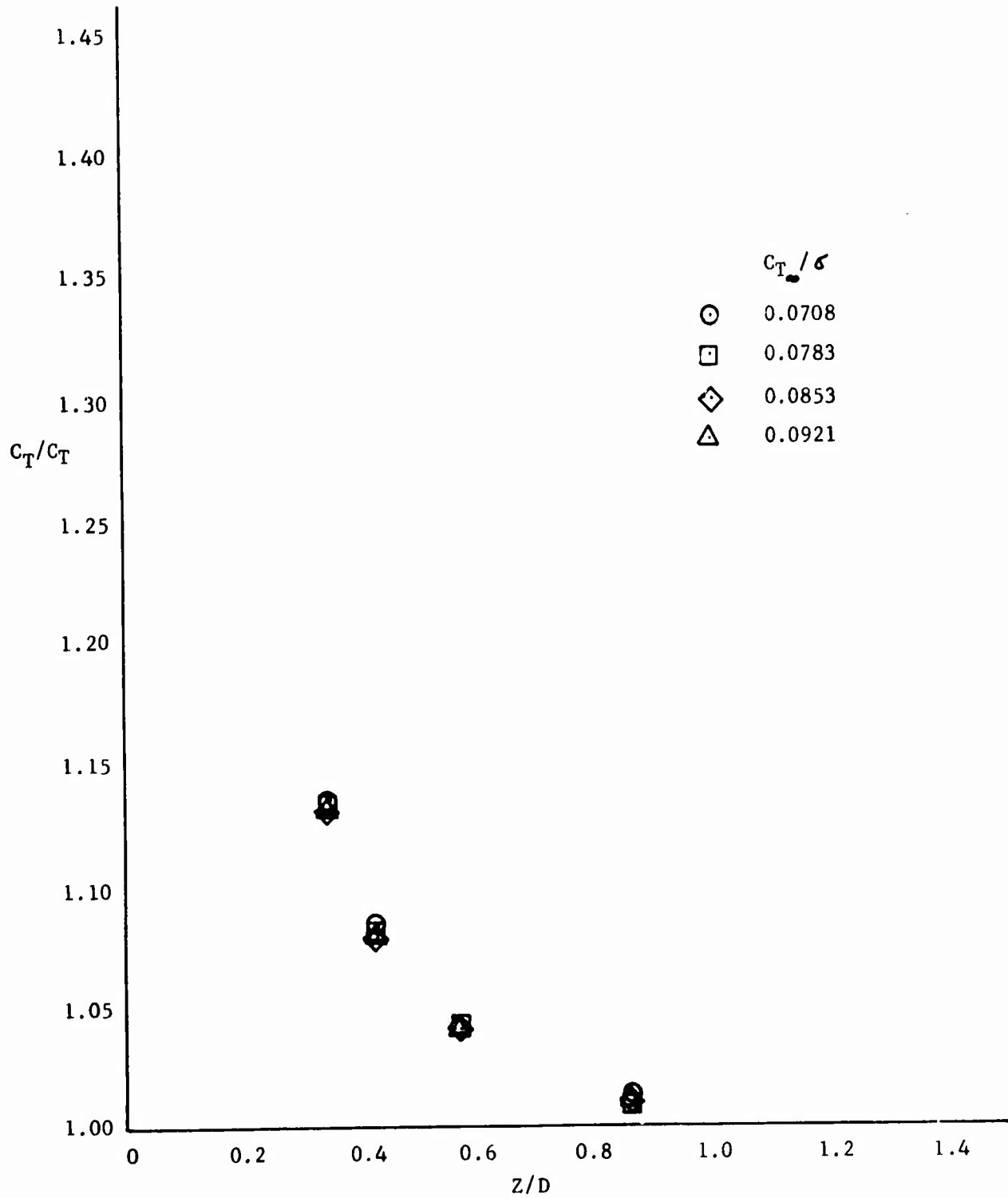
Figure 4

FLIGHT TEST DATA

YH-40
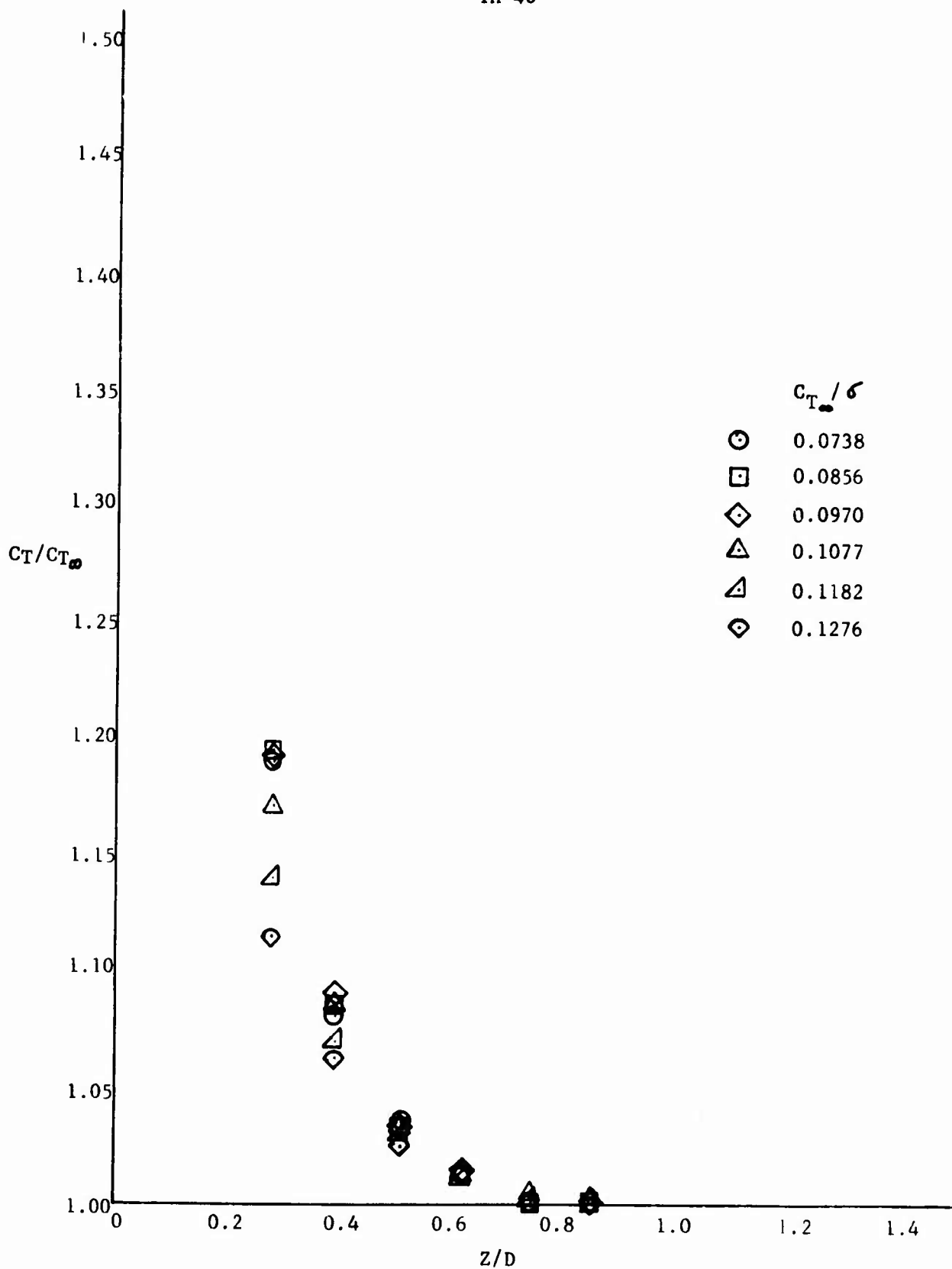
Figure 5

FLIGHT TEST DATA

YHO-2HU

	C_T / σ
⊙	0.0830
⊡	0.0921
◈	0.1005
△	0.1086
◆	0.1165

C_T / C_T

Z/D
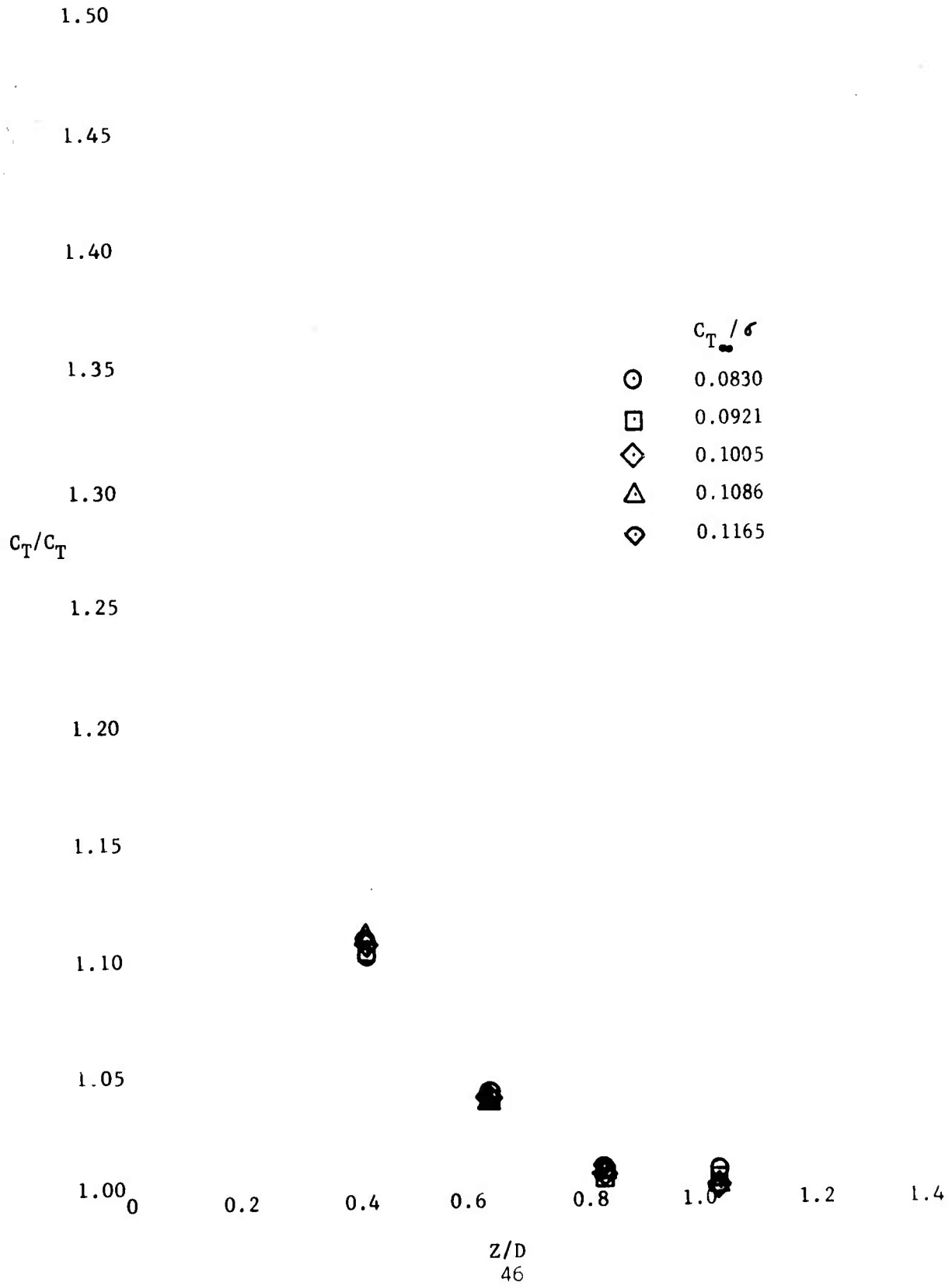
FLIGHT TEST DATA

YUH-1D
(48-Foot Rotor)
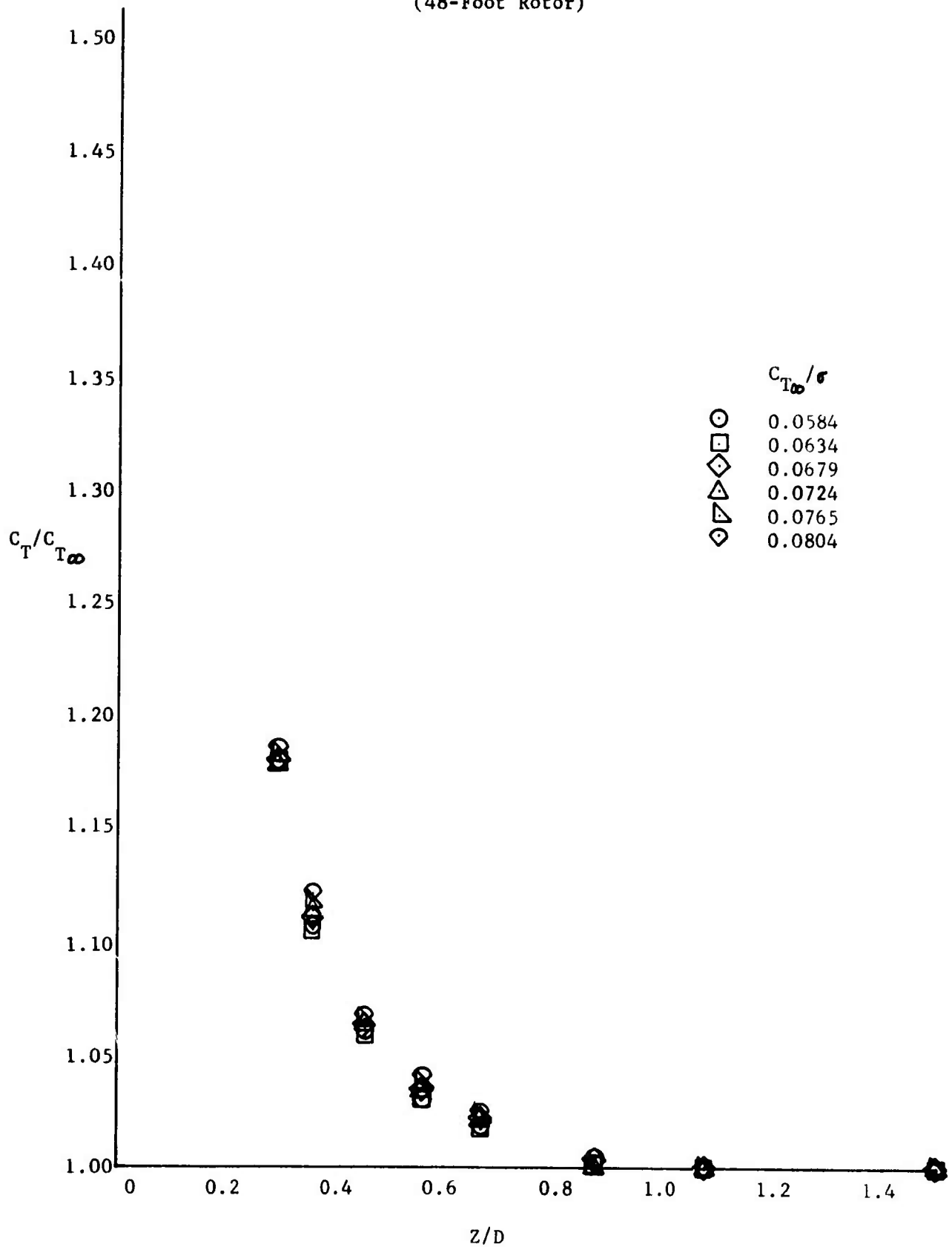
Figure 6

Figure 7

FLIGHT TEST DATA

YUH-1D
(44-Foot Rotor)
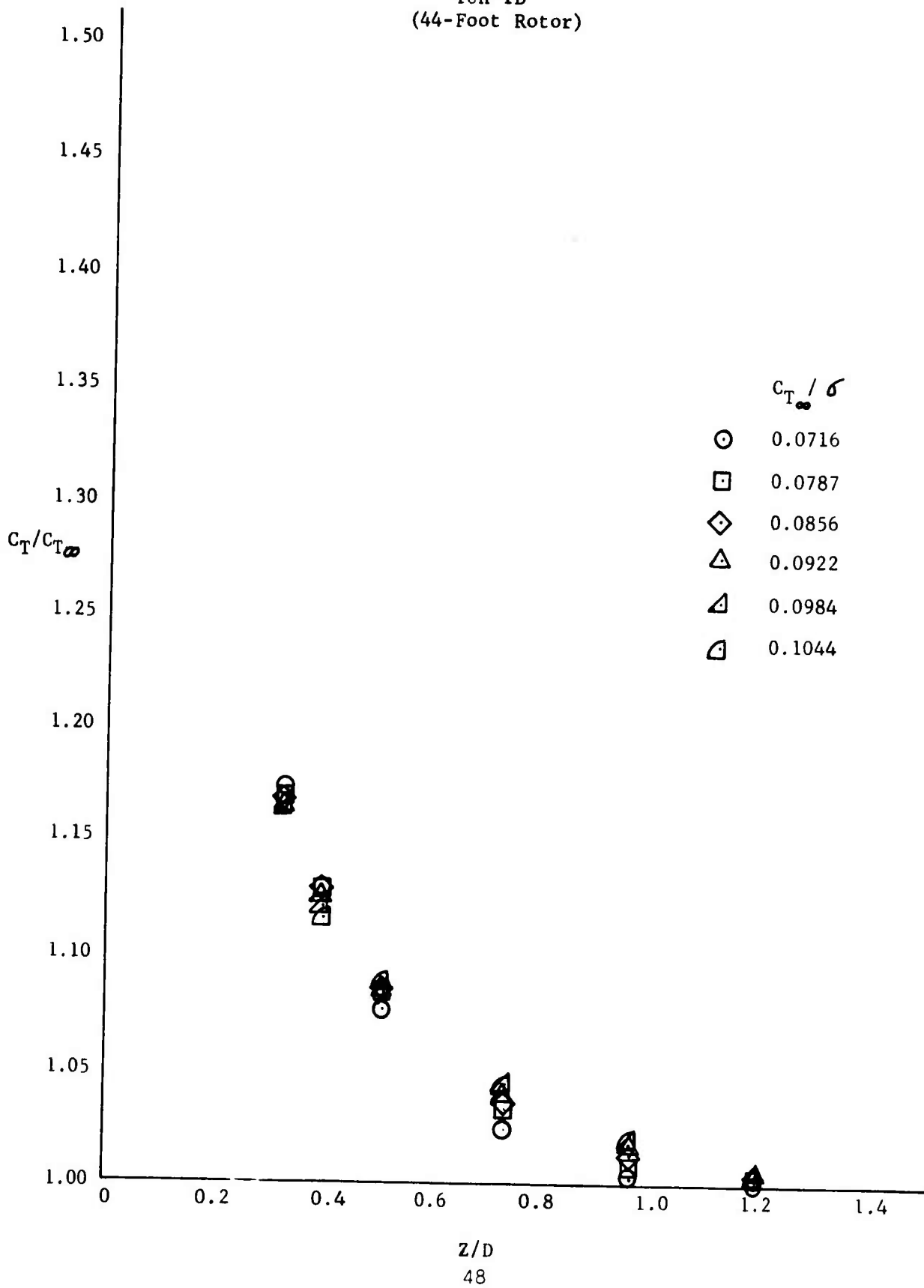
Figure 8

FLIGHT TEST DATA

YHU-1B
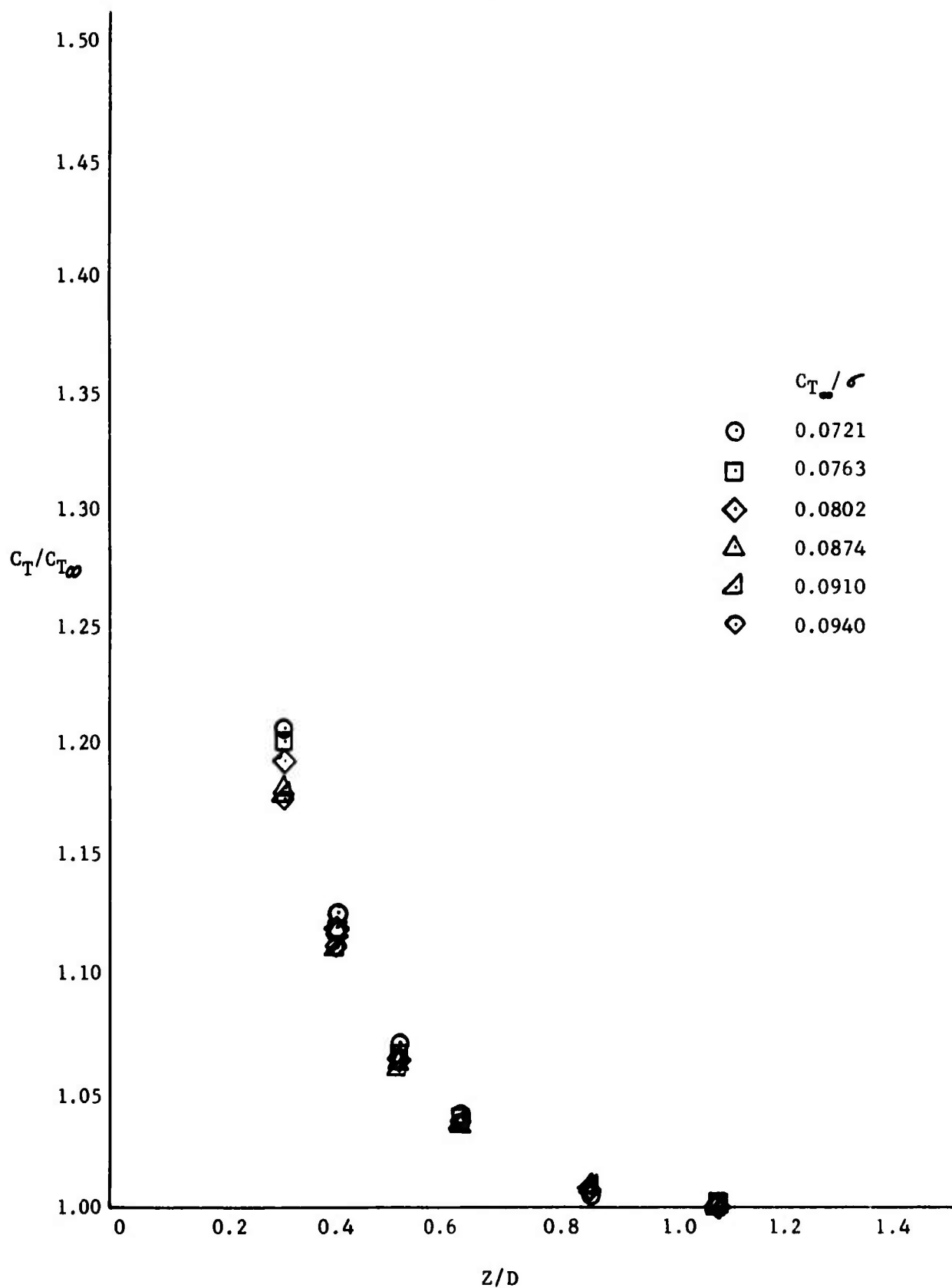
Figure 9

FLIGHT TEST DATA

UH-1C
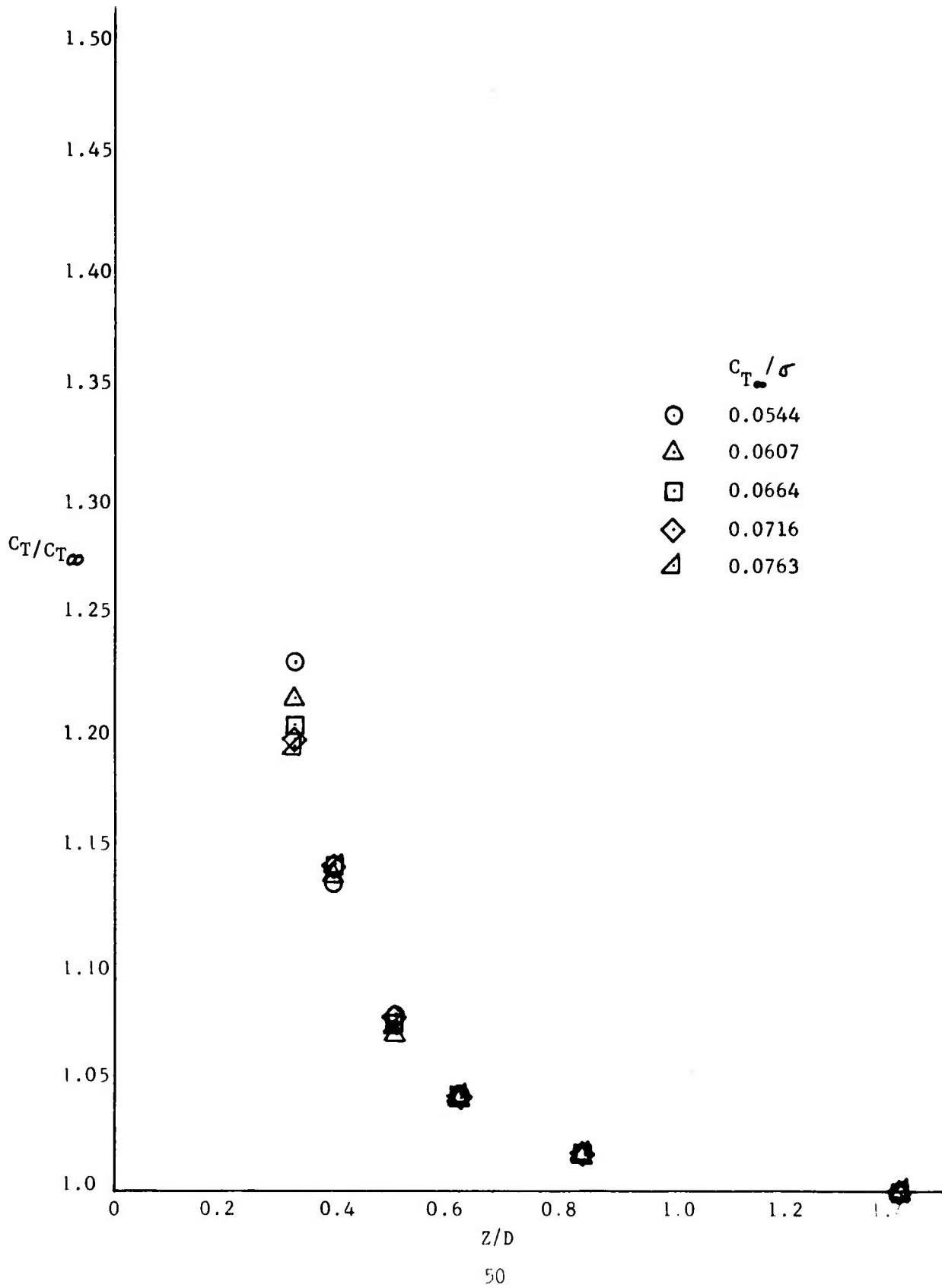
FLIGHT TEST DATA

CH 54-A
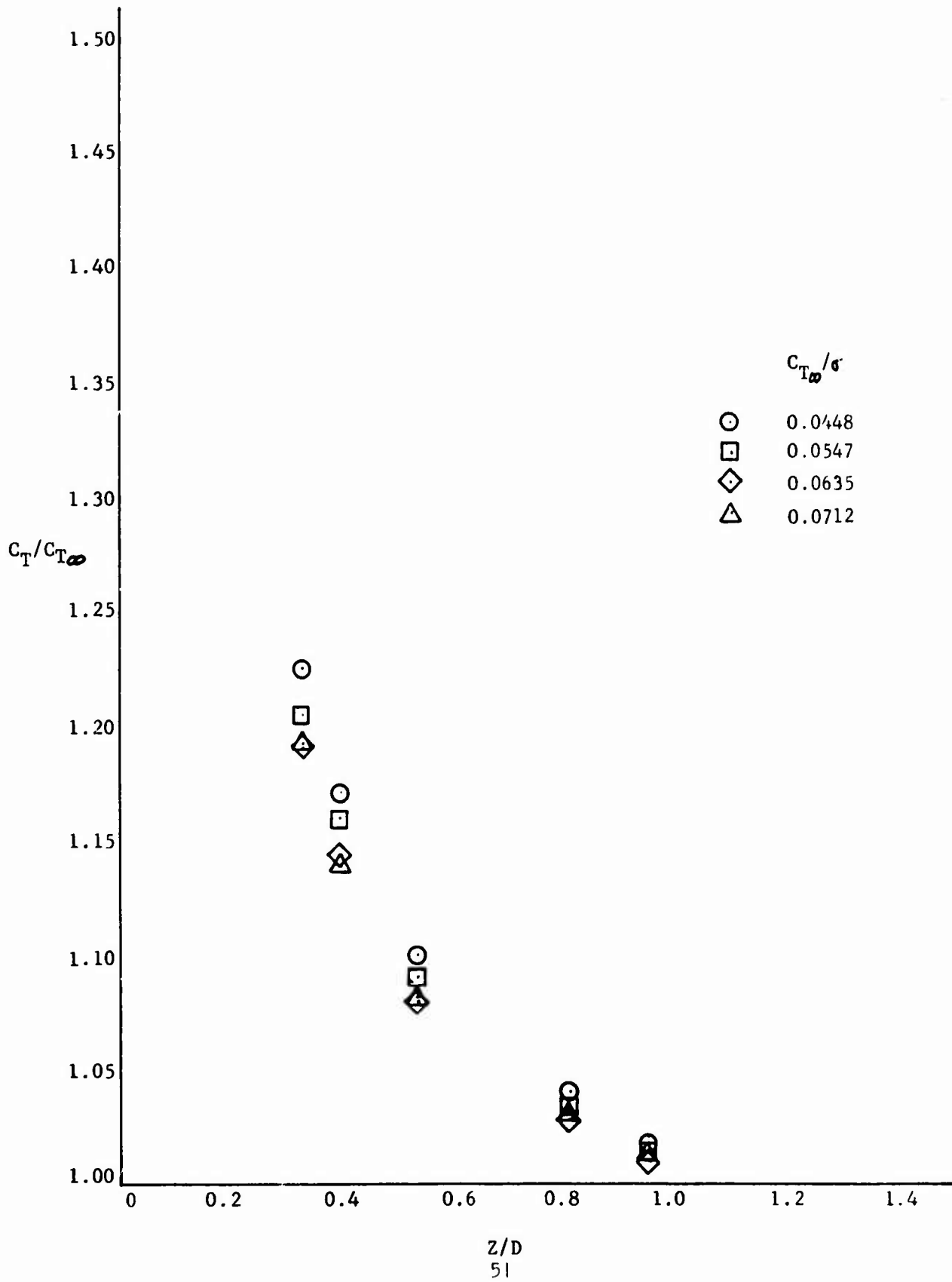
Figure 10

Figure 11

FLIGHT TEST DATA

CH 47-A
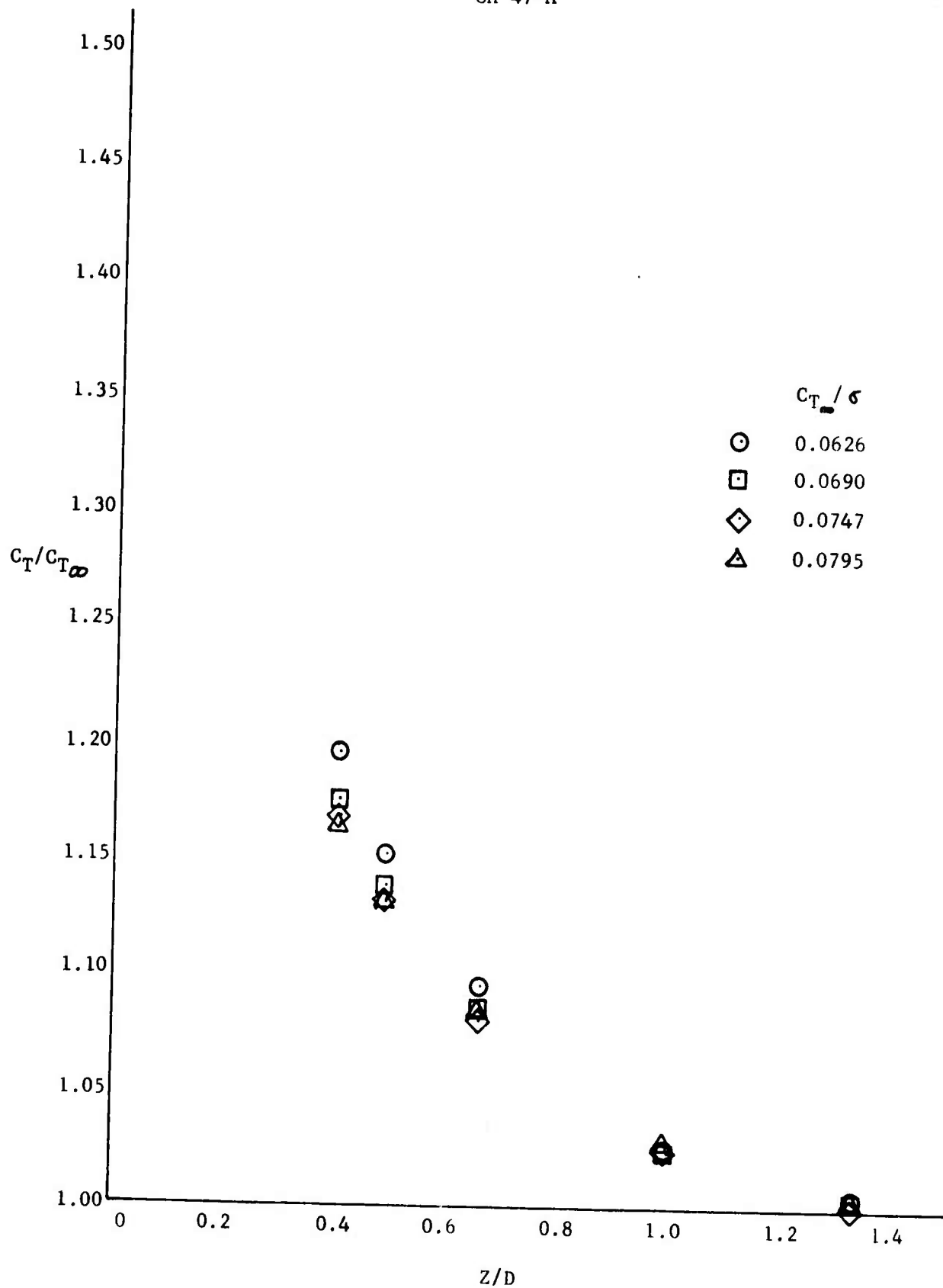
Figure 12

COMPARISON OF MATHEMATICAL FUNCTIONS
FOR SIMULATING FLIGHT TEST DATA

YHU-1B

$C_{T_\infty}/\sigma = 0.0763$

⊙ Flight test data

A: $Y = aX^b$

B: $Y = \dfrac{aX + b}{X}$

C: $Y = \dfrac{X}{aX + b}$

$Y = C_T/C_{T_\infty}$

$X = Z/D$
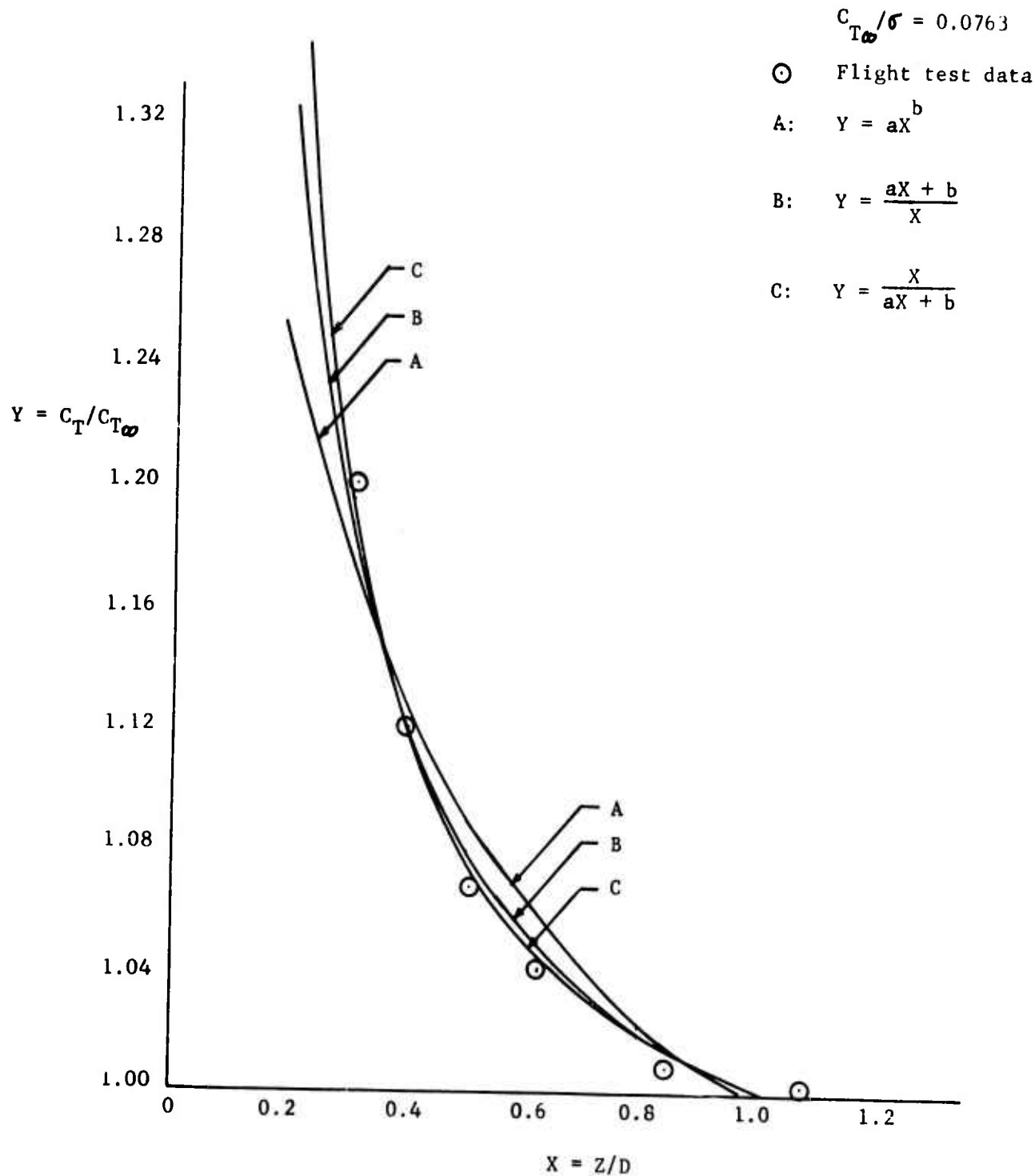
NON-DIMENSIONAL HOVERING PERFORMANCE
YHU-1B

Skid Height = 60 Feet

Figure 13

54
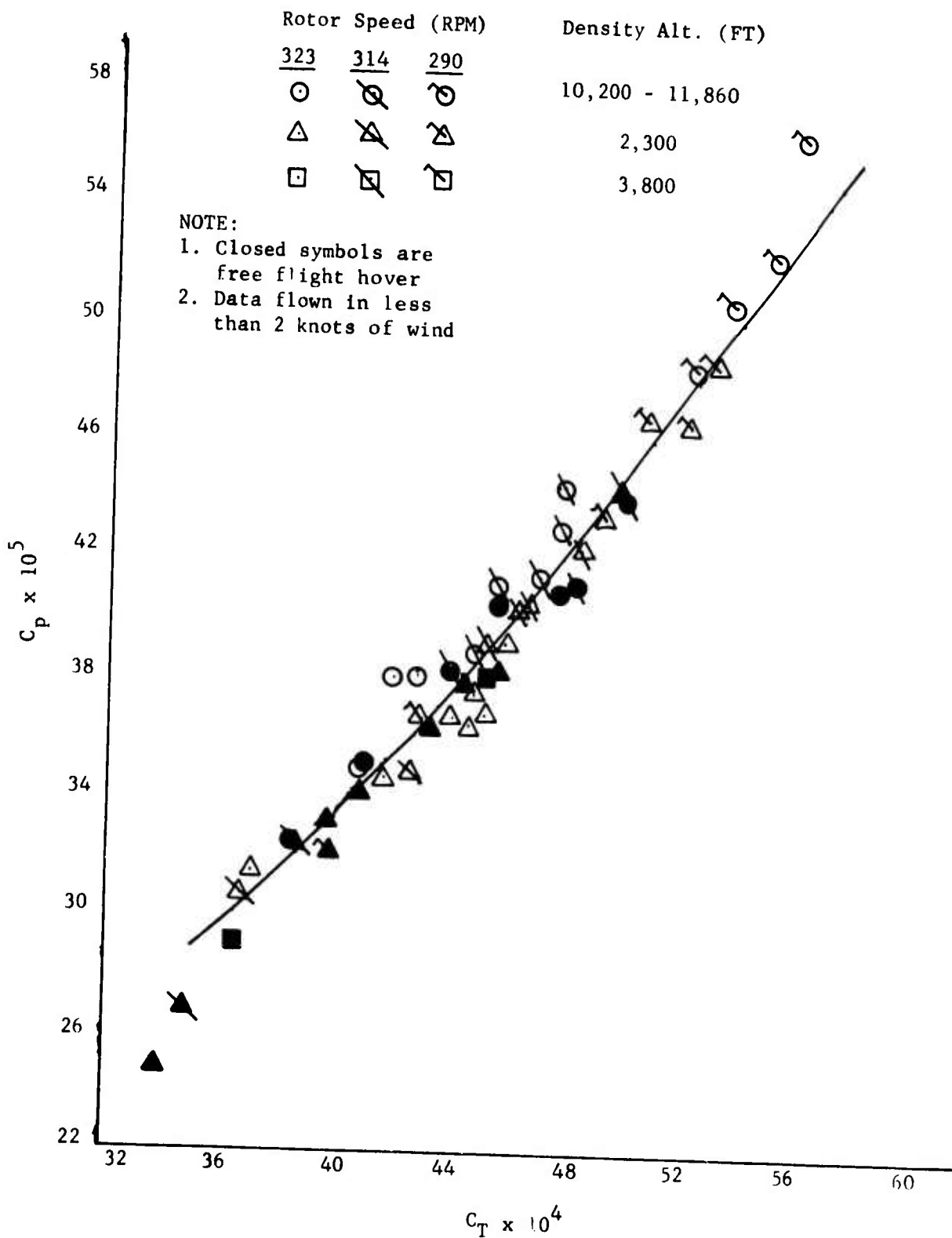
Figure 14

EFFECT OF DATA SELECTION ON
LEAST SQUARES APPROXIMATION

YUH-1D

$C_{T_\infty}/\sigma = 0.0634$

⊙ Flight test data

A: Excluding data points for
which $C_T/C_{T_\infty} = 1.0$

B: Excluding data point for
which $Z/D = 1.5$

C: Including all data points
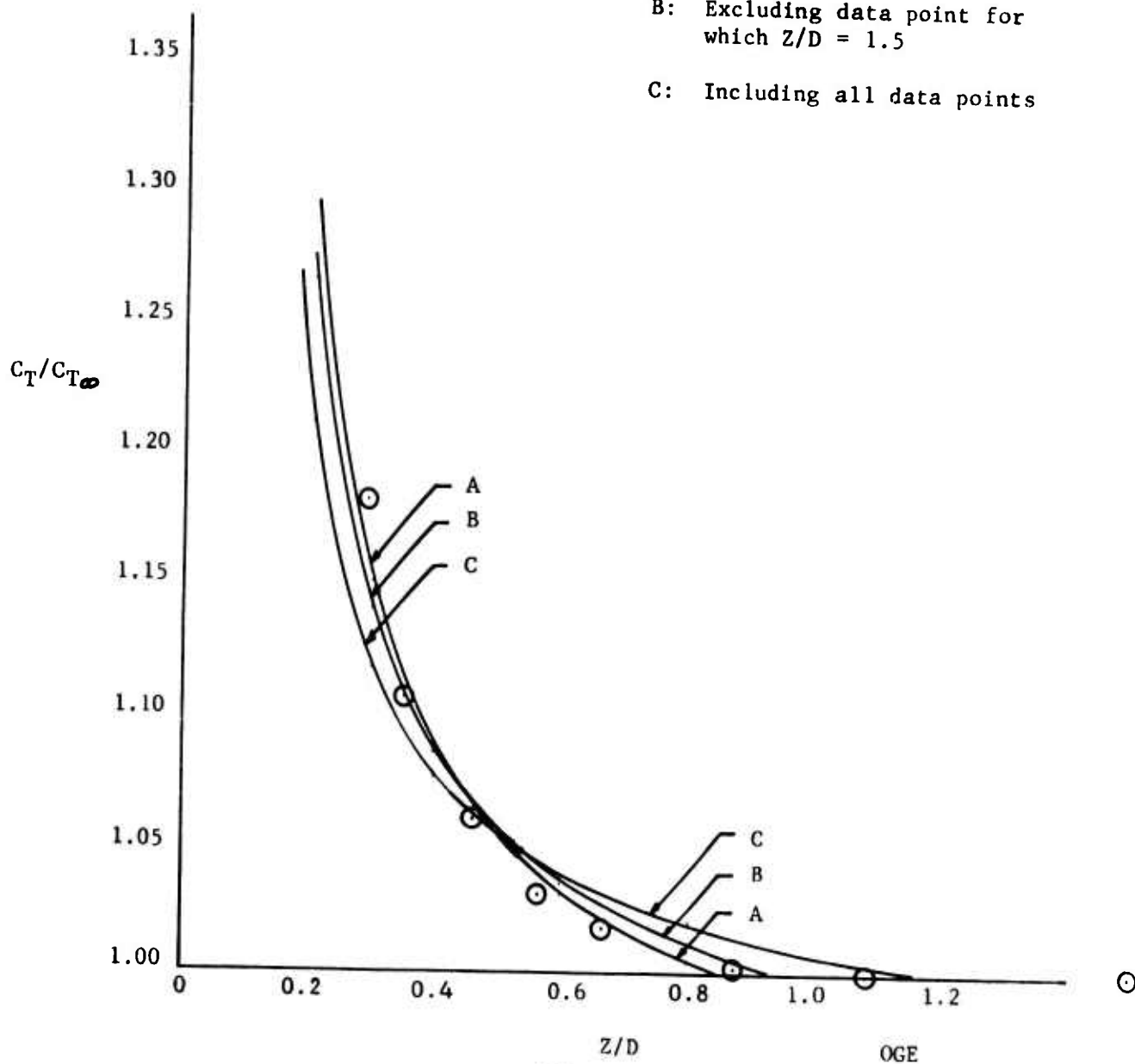
DISTRIBUTION OF VALUES OF a
and
LEAST SQUARES FIT OF a AS FUNCTION OF $C_{T\omega}/\sigma$

Figure 15

$a = 1.099107 - 0.289447 \ (C_{T\omega}/\sigma)$

Legend:
- ⊙ Bell 47 J-2
- ◁ CH-47A
- □ UH 12E-4
- ⧀ YUH-1D (48 ft)
- ◇ CH-54A
- ◇ YHO-2HU
- ◁ YH-40
- ◇ YUH-1D (44 ft)
- ◁ YHU-1B
- ◁ UH-1C

56
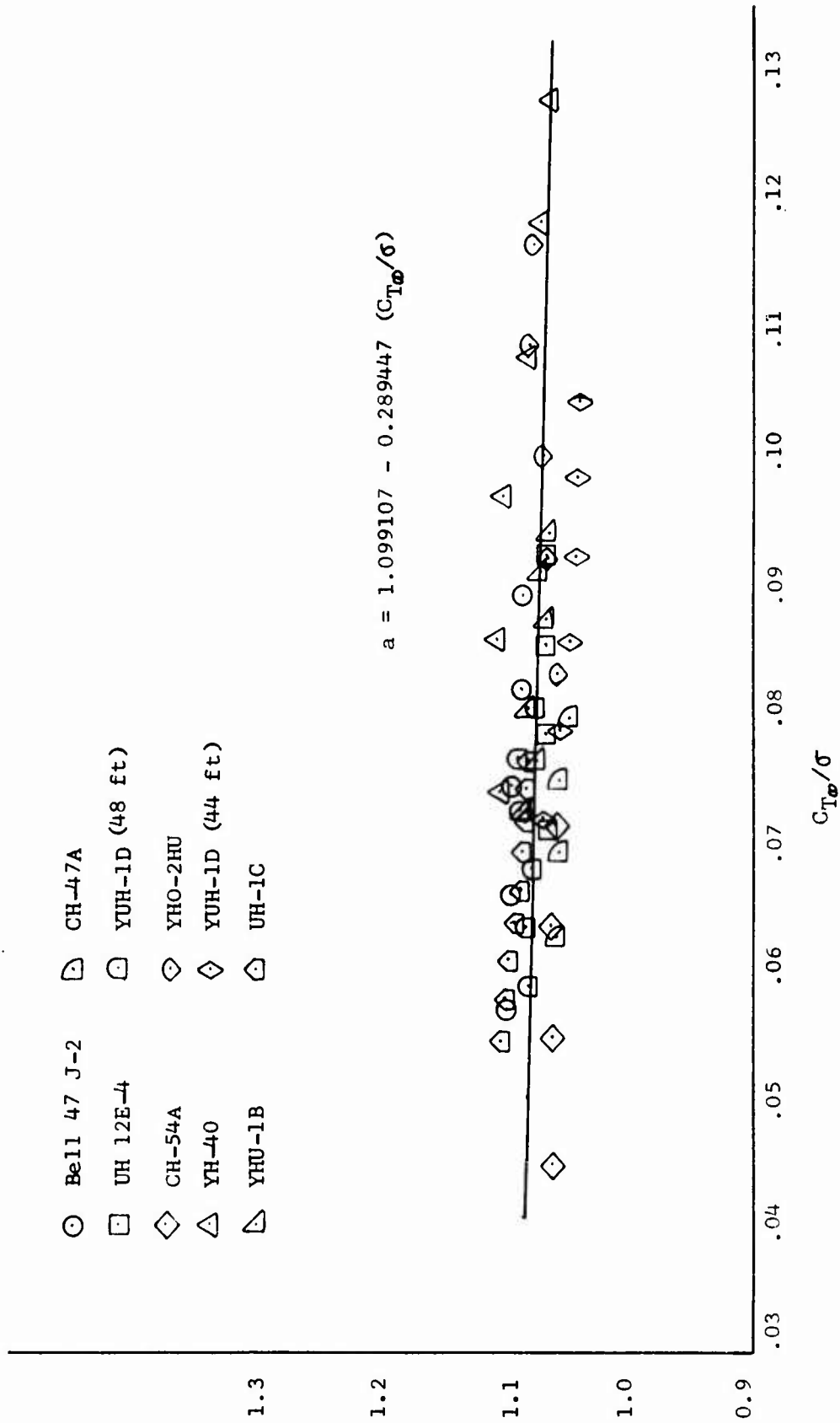
DISTRIBUTION OF VALUES OF b
and
LEAST SQUARES FIT OF b AS FUNCTION OF $c_{T\omega}/\sigma$

$b = -0.104183 + 0.391397 \, (c_{T\omega}/\sigma)$

Figure 16

57
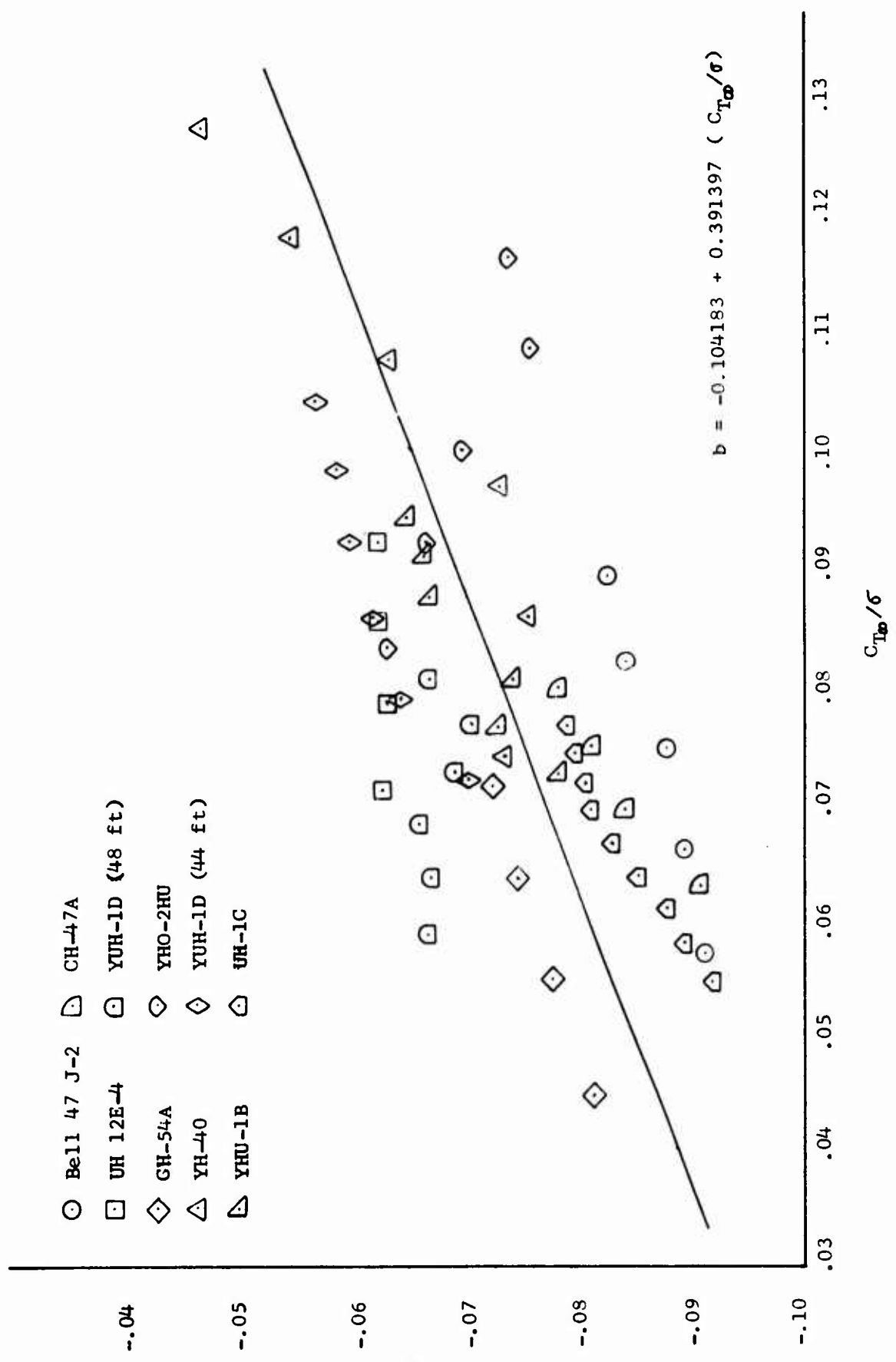
Figure 17

HOVERING PERFORMANCE
by the
GENERALIZED EQUATION (4.1)
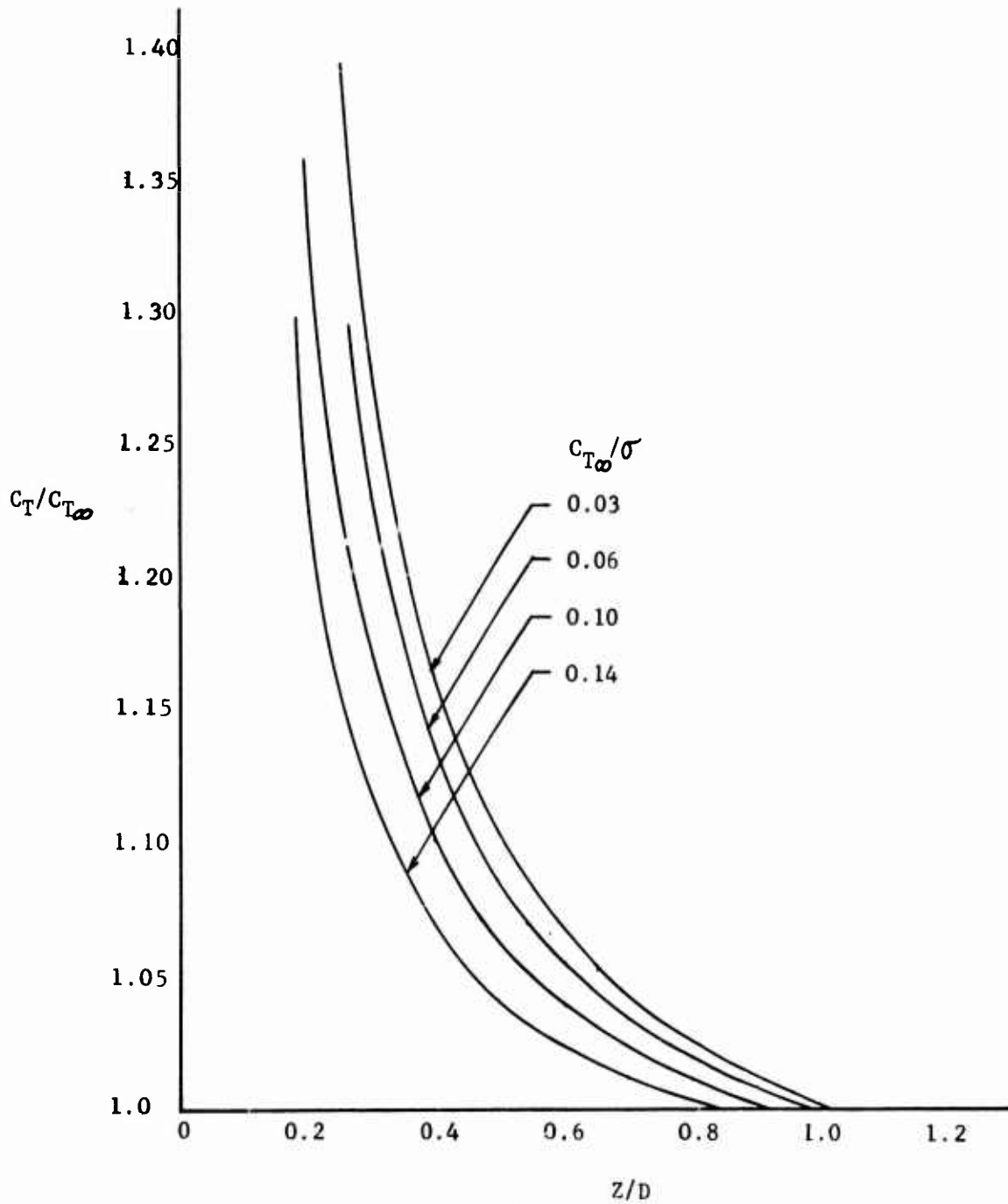
Figure 18

COMPARISON OF THE PREDICTED AND FLIGHT
HOVERING PERFORMANCE
FOR
YUH-1D (44 ft rotor)
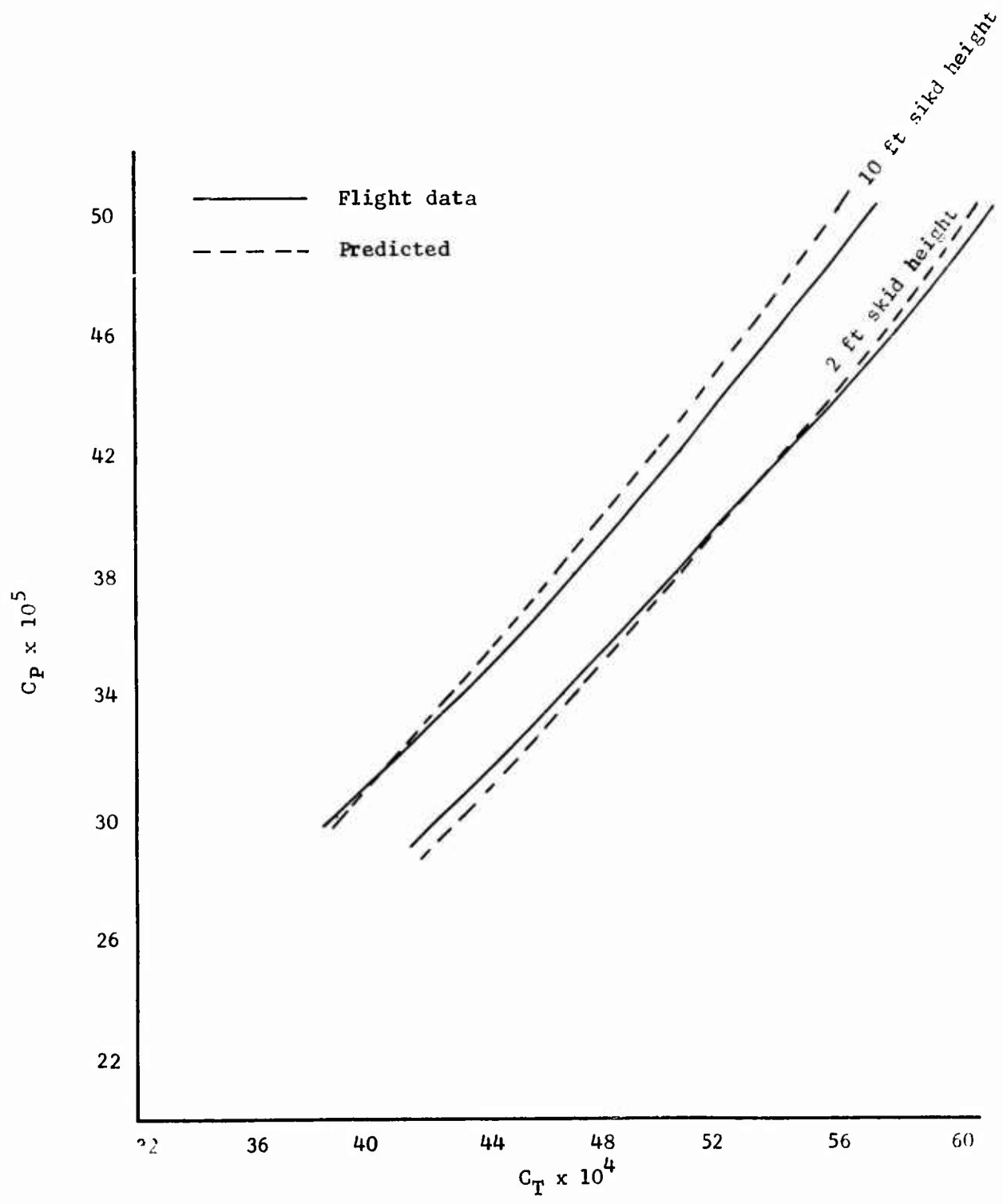
Figure 19

DISTRIBUTION OF PERCENTAGE DEVIATION
OF PREDICTED C_T/C_{T_∞} FROM FLIGHT DATA

Standard deviation = 2.0891
Sample mean = -0.3641

FREQUENCY

PERCENTAGE DEVIATION
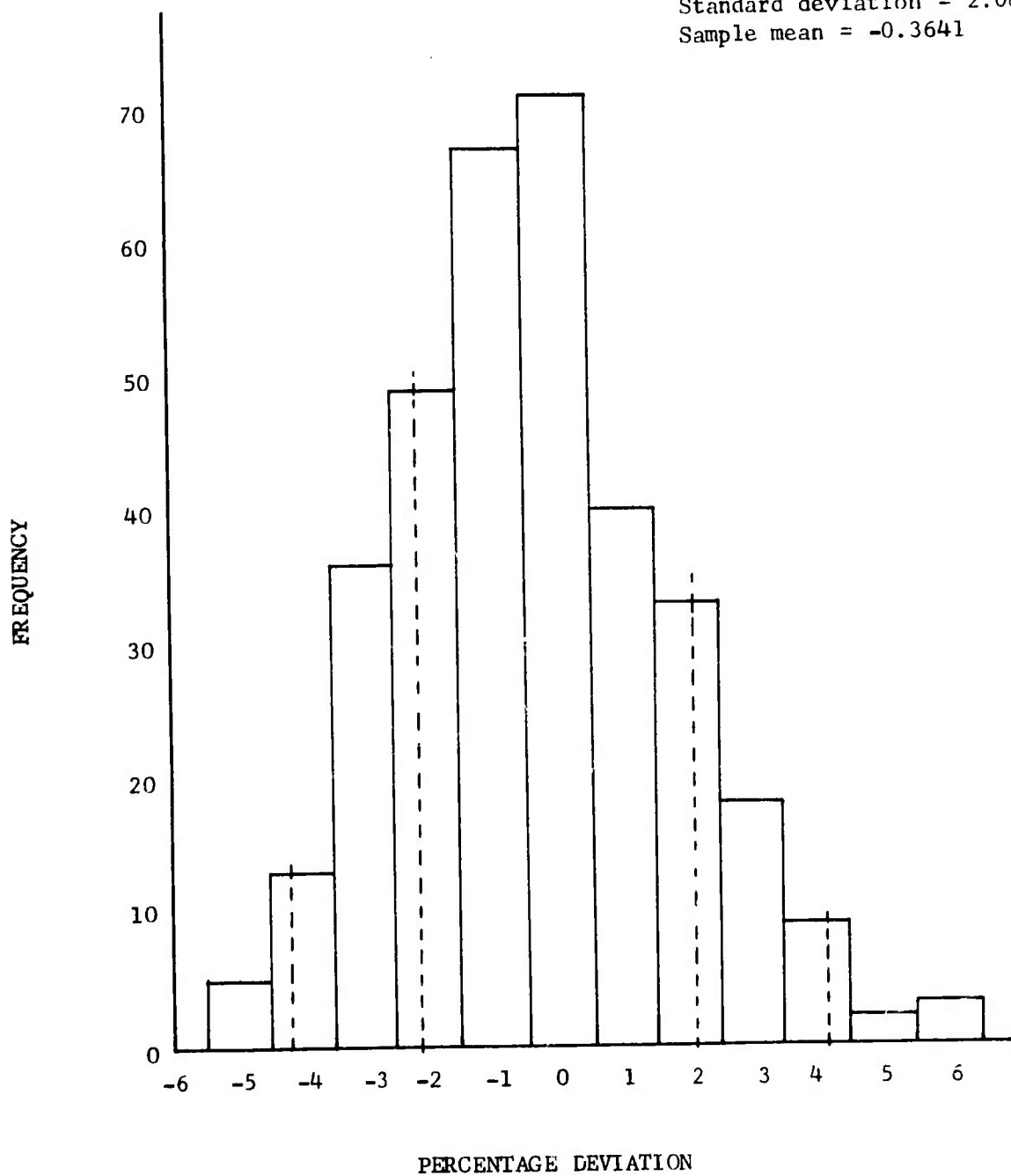
Figure 20

PROBABILITY OF PERCENTAGE DEVIATION OF
PREDICTED C_T/C_{T_∞} FROM FLIGHT DATA

Standard deviation s=2.0891
Sample mean   m = -0.3642

PROBABILITY

PERCENTAGE DEVIATION

61
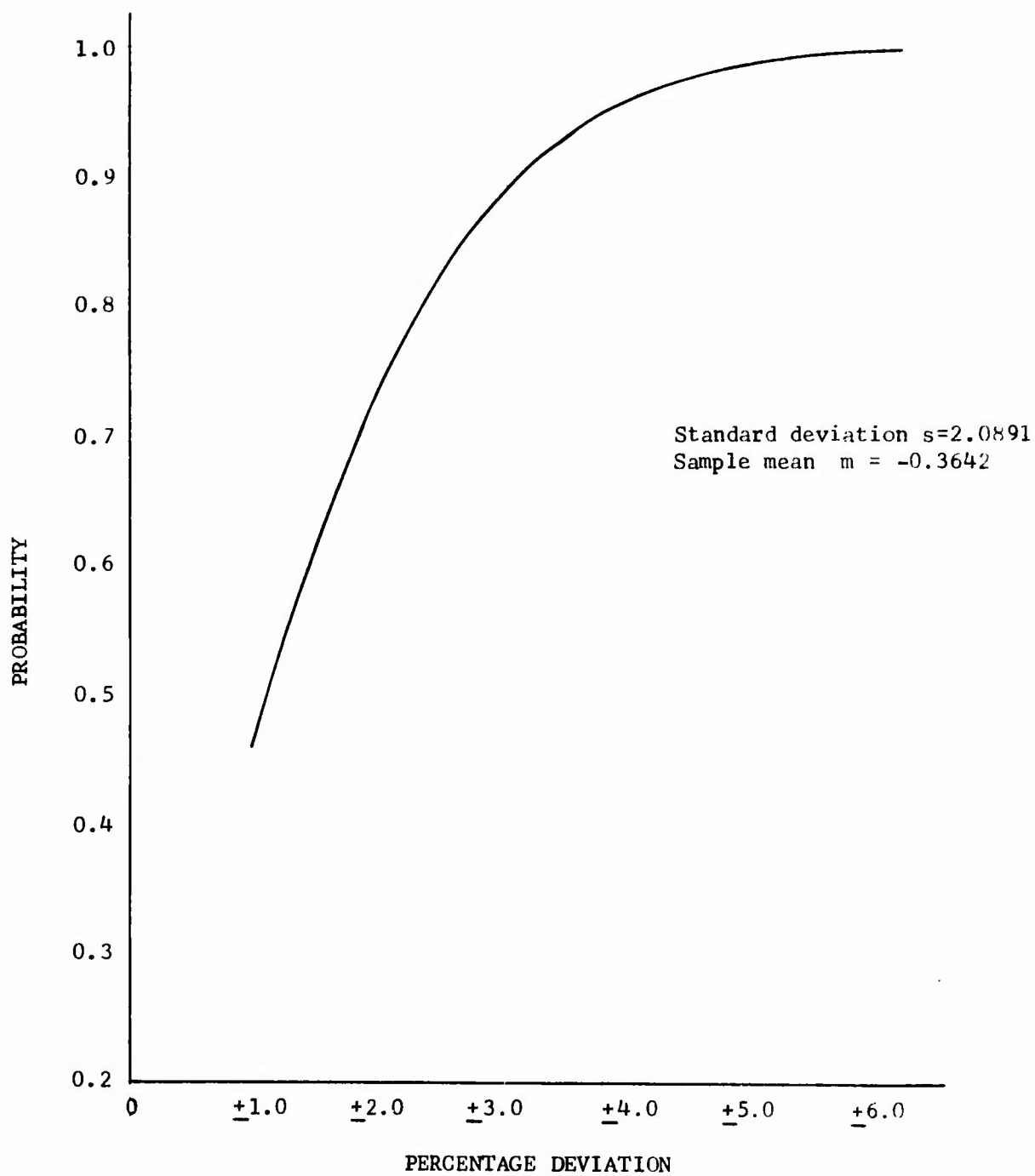
Figure 21

COMPARISON OF PREDICTED AND FLIGHT
HOVERING PERFORMANCE
OF

OH-6A
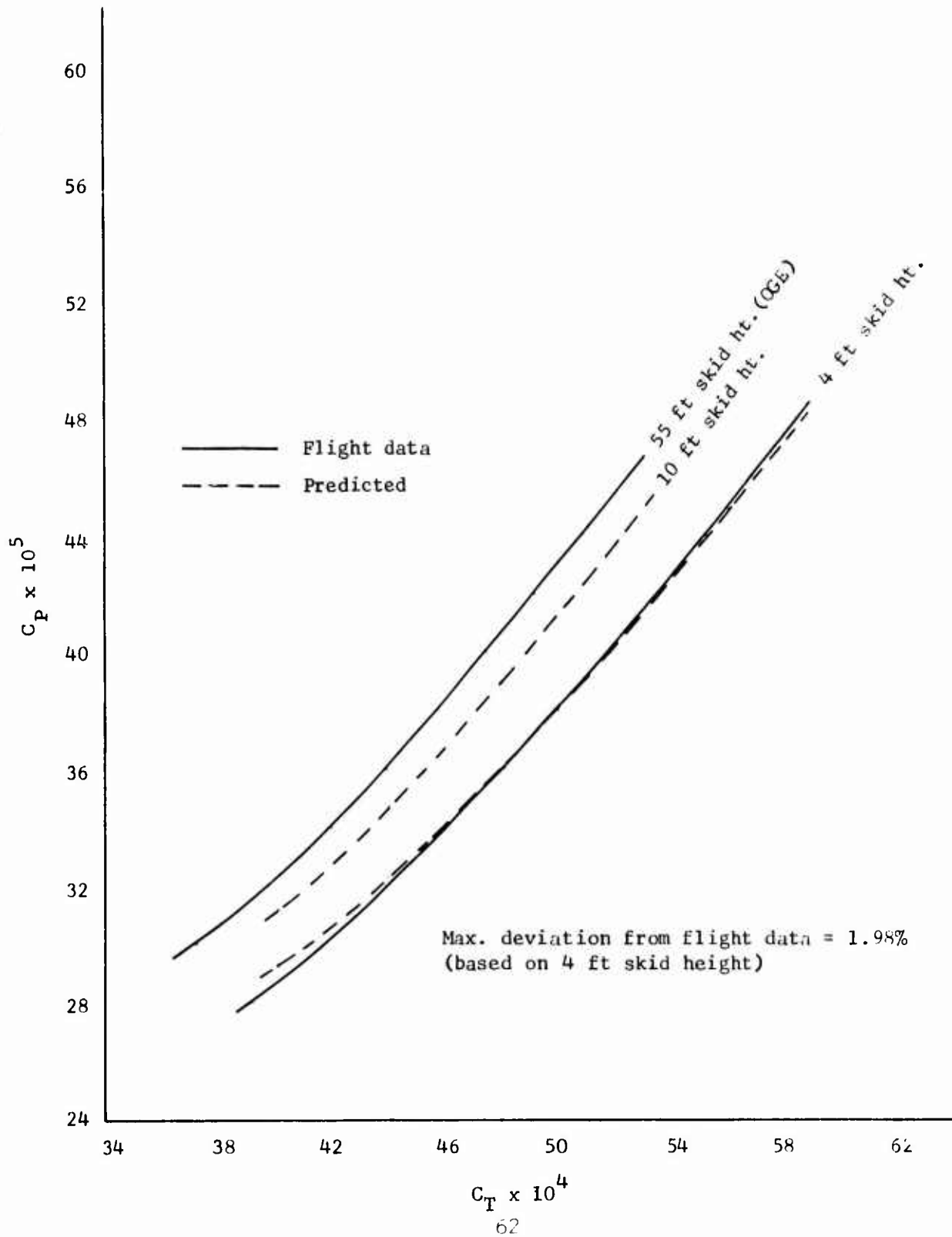
COMPARISON OF PREDICTED AND FLIGHT
HOVERING PERFORMANCE
OF

LOH 206A

Figure 22

63
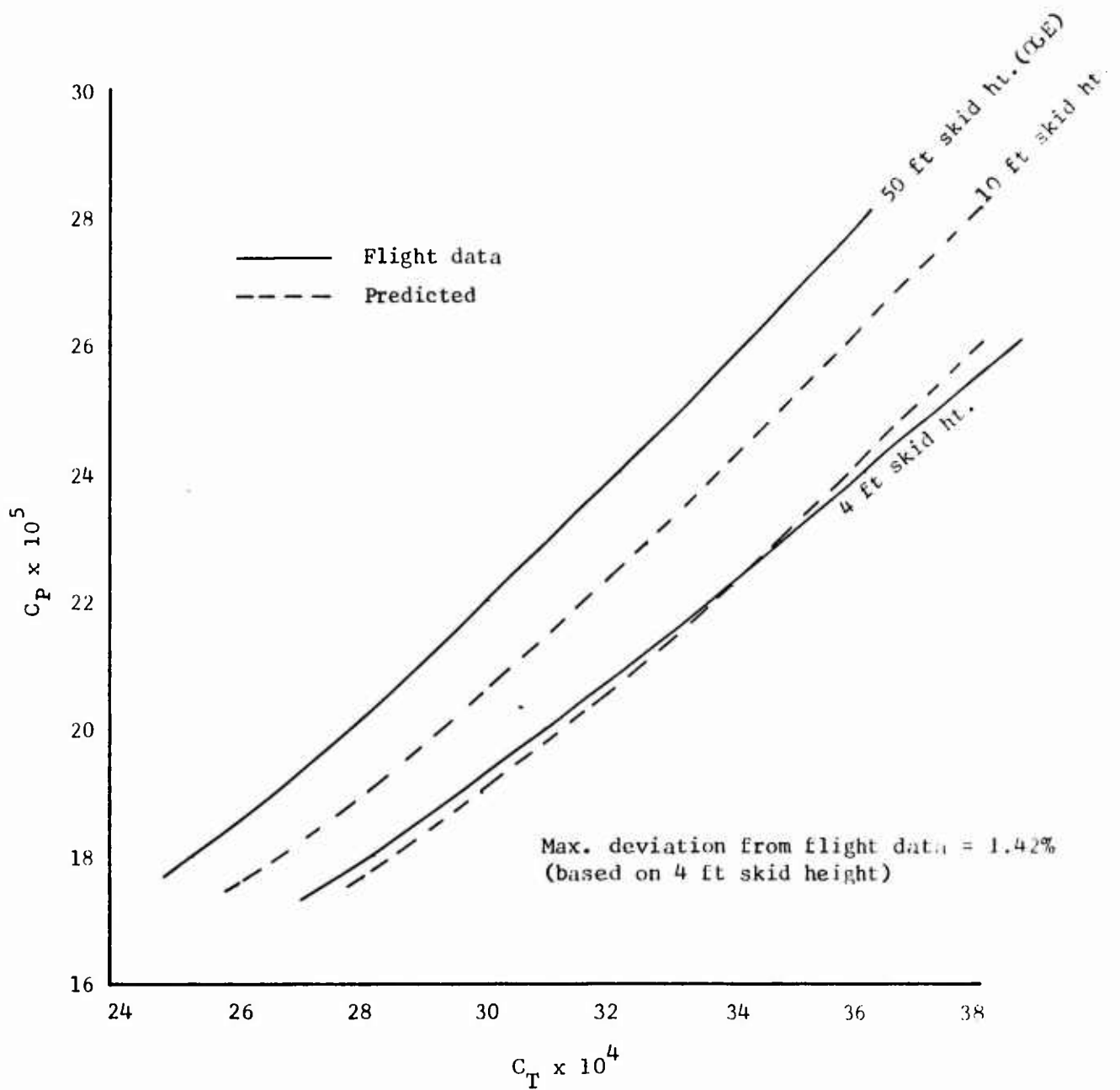
COMPARISON OF PREDICTED AND FLIGHT
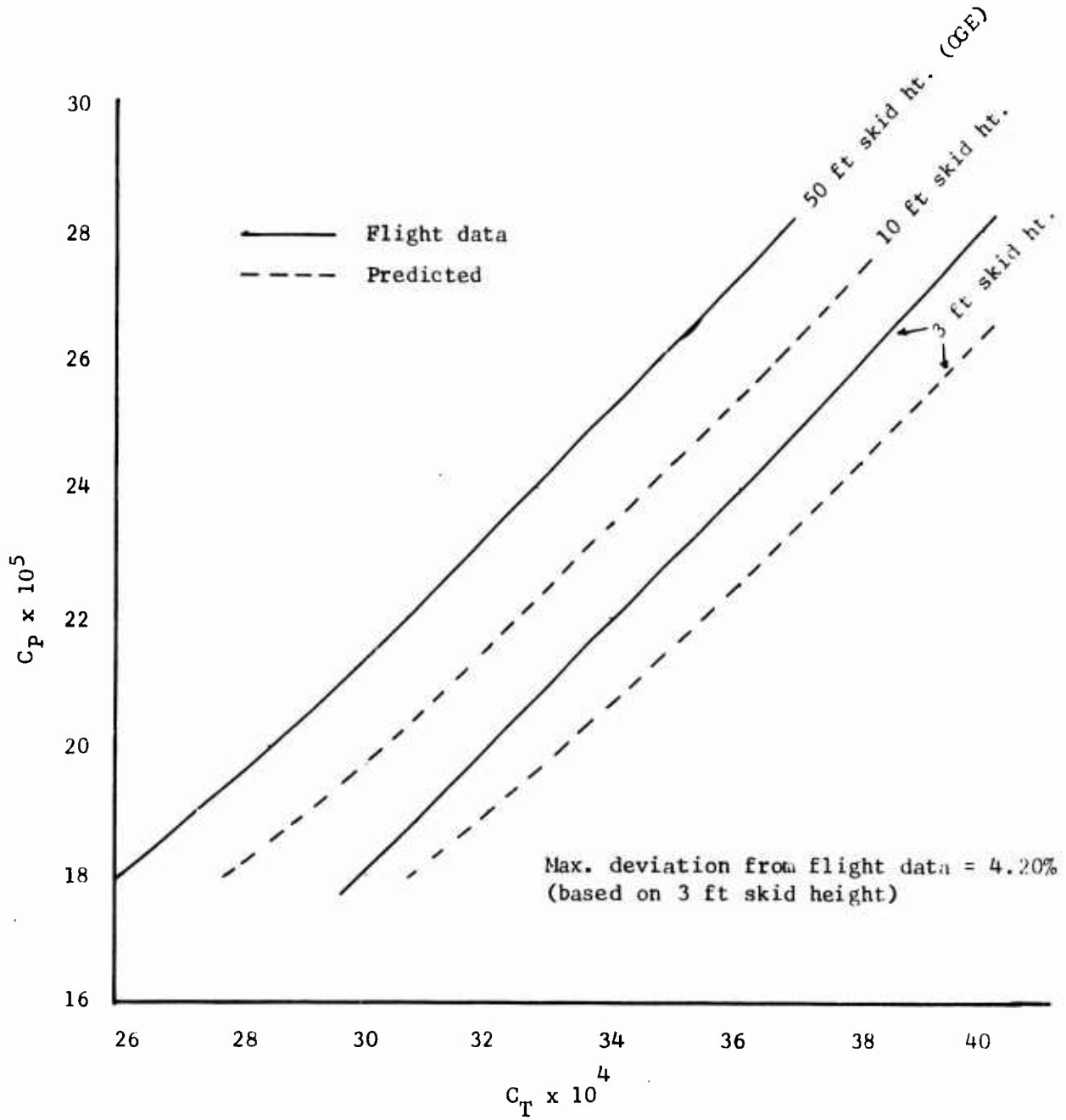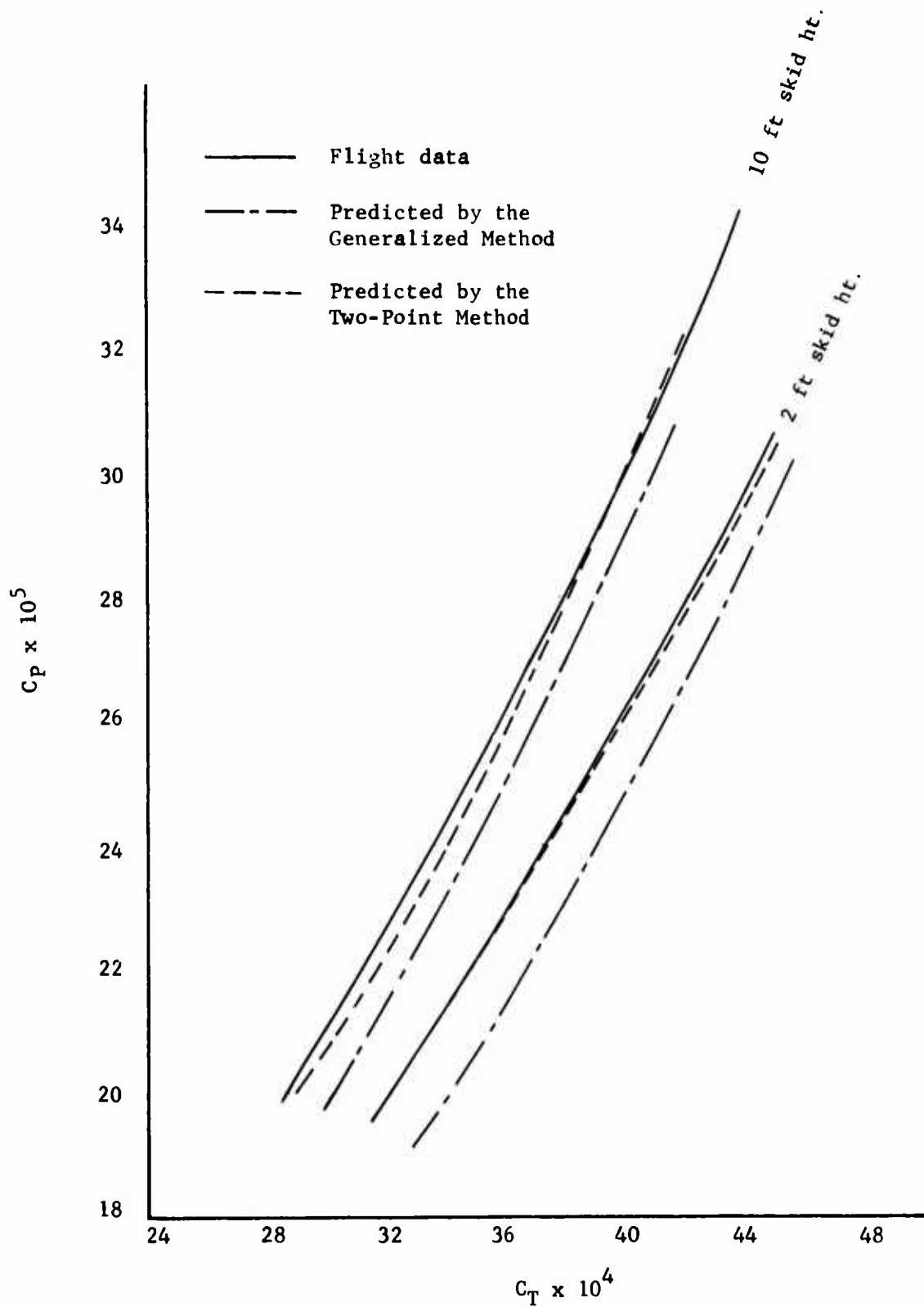HOVERING PERFORMANCE
OF

AH-1G

Figure 23
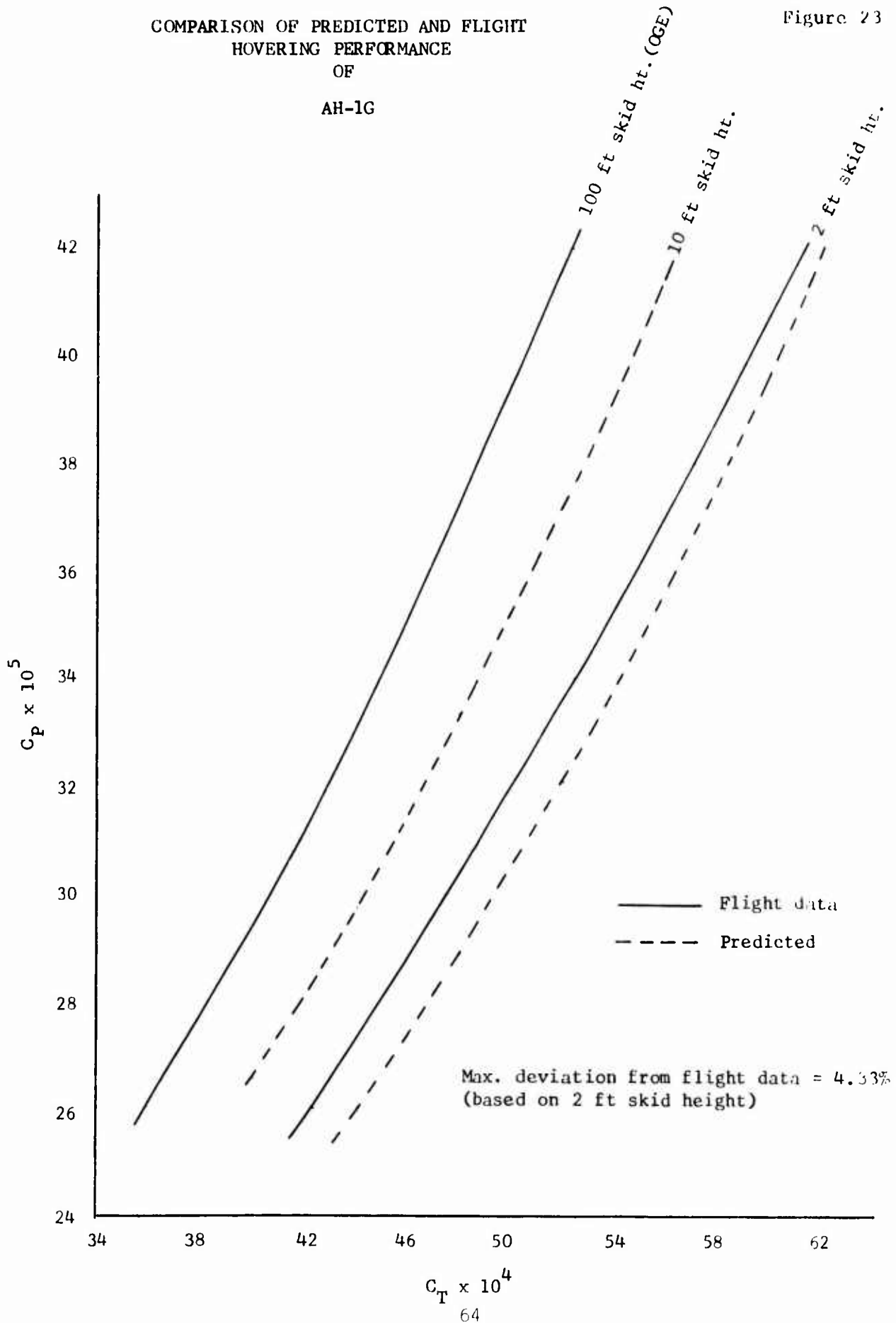
COMPARISON OF PREDICTED AND FLIGHT
HOVERING PERFORMANCE
OF

YH-41

Figure 24

65

COMPARISON OF METHODS OF PREDICTION
for
YUH-1D (48 ft rotor diameter)

Figure 25

66

Figure 26

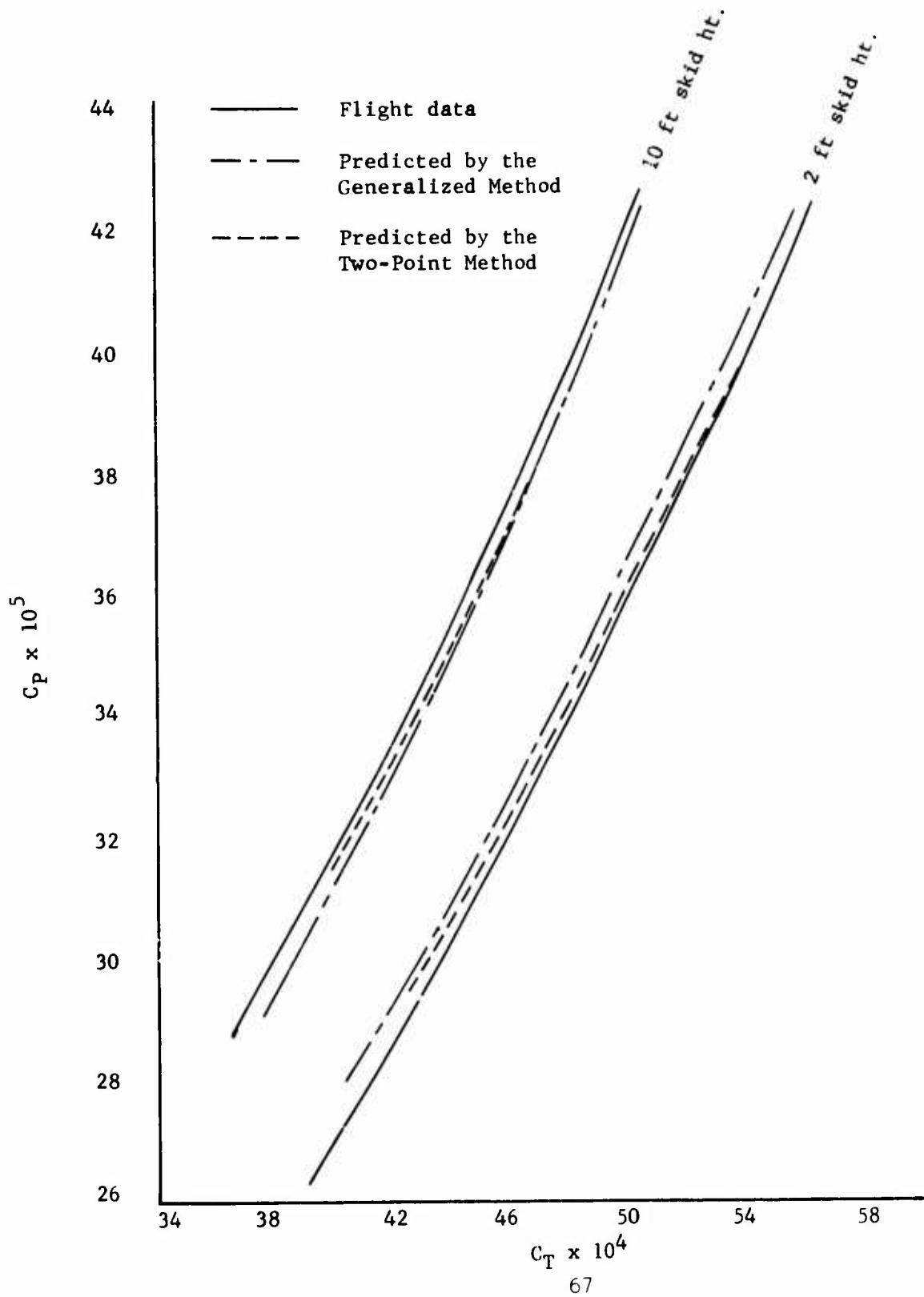COMPARISON OF METHODS OF PREDICTION
for
UH-1C

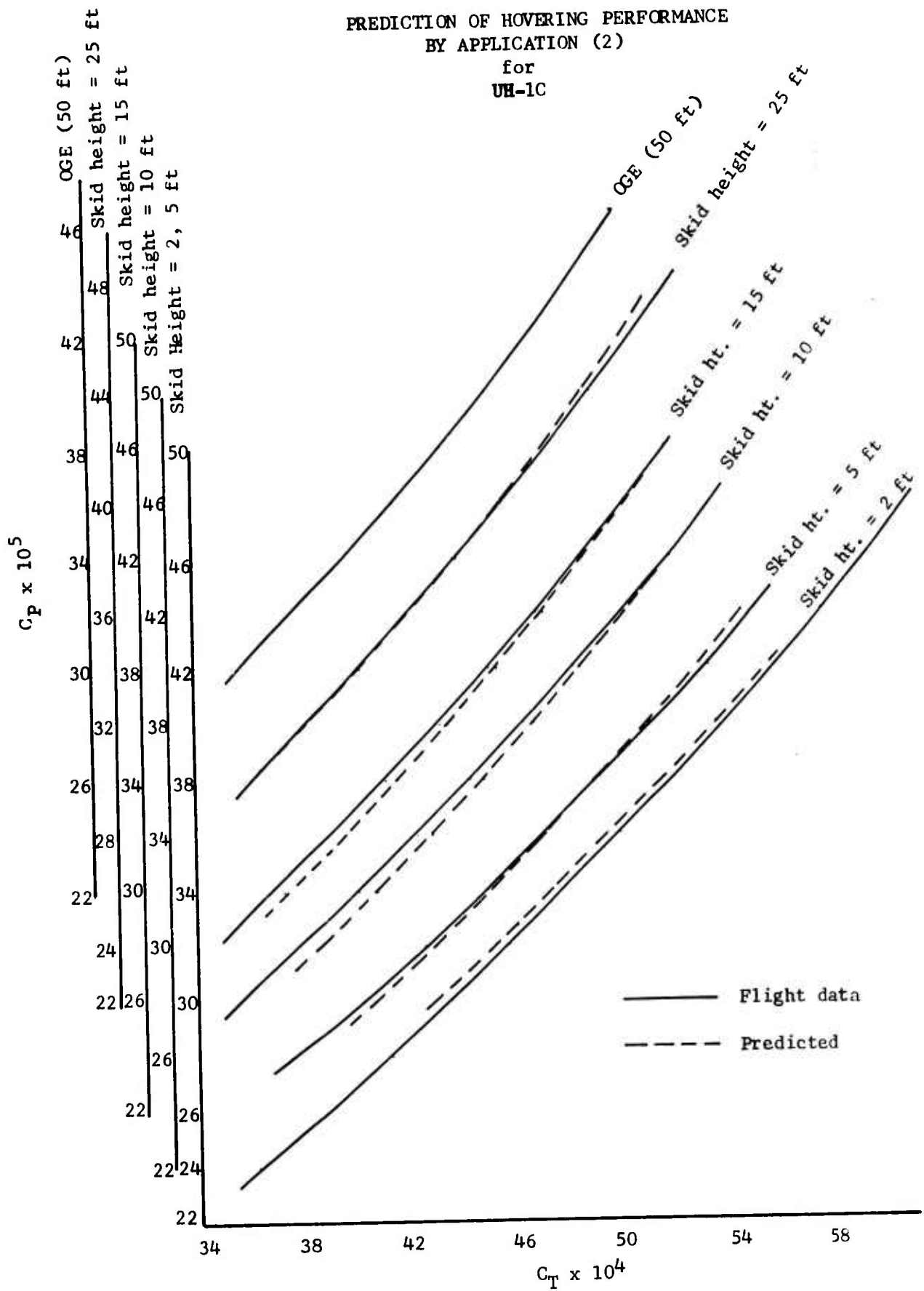**PREDICTION OF HOVERING PERFORMANCE**
BY APPLICATION (2)
for
UH-1C

PREDICTION OF HOVERING PERFORMANCE
BY APPLICATION (5)
for
UH-1C

$C_P \times 10^5$

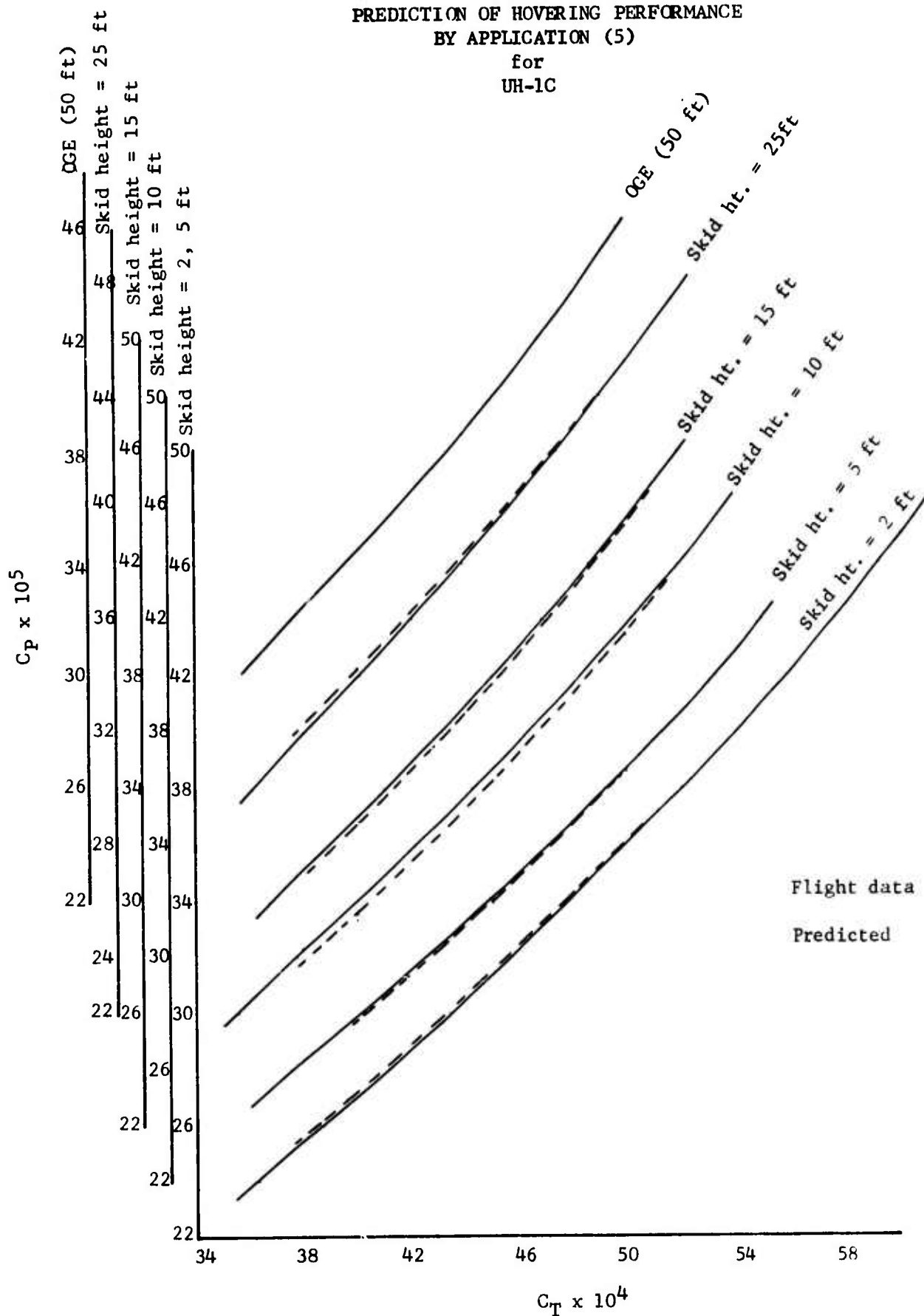$C_T \times 10^4$

Flight data

Predicted

LINEAR GRAPHICAL TEST FOR THE
SUITABILITY OF EMPIRICAL FUNCTIONS

Figure B-1

YHU-1B

$(C_{T_\infty}/\sigma = 0.0763)$

⊙ Flight test data

$Y = aX^b$

$Y = C_T/C_{T_\infty}$

$X = Z/D$

log Y

log X

$X = Z/D$

$Y = C_T/C_{T_\infty}$

X/Y
or
XY

$Y = \dfrac{X}{aX + b}$

$Y = \dfrac{aX + b}{X}$

△, □ Flight test data

$X = Z/D$